GA-A15197

FISSION PRODUCT RELEASE AND TRANSPORT IN GAS-COOLED FAST BREEDER REACTOR SEALED AND VENTED IRRADIATION EXPERIMENTS

by

S. LANGER, G. BUZZELLI, J. R. LINDGREN,
P. W. FLYNN, R. J. CAMPANA, L. NEIMARK,*
S. GREENBERG,* and C. E. JOHNSON*

This is a preprint of a paper to be presented at the International Conference on Fast Breeder Reactor Performance, March 5-8, 1979, Monterey, California. A condensed version of this report will be published in the Proceedings.

Work supported by
Department of Energy
Contract EY-76-C-03-0167, Project Agreement No. 23

*Argonne National Laboratory, Argonne, Illinois

GENERAL ATOMIC PROJECT 6113
NOVEMBER 1978

GENERAL ATOMIC COMPANY

CONTENTS

FIGURES

TABLES

INTRODUCTION

The vented and pressure-equalized design of gas-cooled fast breeder reactor (GCFR) fuel rods and subassemblies has been studied for several years[1-3]. The vented design imposes on the reactor designer the requirement of being able to predict the behavior and transport of all important gaseous and volatile radionuclides so that their expected distribution in the plant may be used for component design and safety analysis. An overly conservative system design, based on the absence of an adequate data base for fission product release, is uneconomical and impractical. Thus, for each important mass chain, knowledge of the release of the various chain nuclides from the fuel and their transport, plateout, and interactions in the fuel rod, subassembly, pressure equalization system (PES), and helium purification system (PES) is essential. This paper describes the irradiation experiment data base from which information on the transporting species and the transported fractions of volatile and gaseous species is obtained. The data are analyzed to define the predominant transporting mechanism for the nuclides in each mass chain.

The GCFR irradiation program has used vented single rod irradiations with unique piping arrangements to obtain detailed information on the transport of fission gas radionuclides in the vented fuel rod during the operational phase of irradiation. In some instances, migration of the halogen precursor of the noble gas has also been measured. Data on end-of-life distributions of the alkali and alkaline earth metal daughters of the noble gases can be obtained during postirradiation examination.

To date, fast flux irradiations have been limited to sealed rods in EBR-II, although a vented, prototypical 12-rod bundle is currently operating in an epithermal flux under typical GCFR conditions in the BR-2 reactor at Mol[4]. Extensive gamma spectrometry on the fuel rods, coupled

with chemical and radiochemical analysis of the fuel and blanket pellets and the charcoal traps during postirradiation examination, has yielded data from which the predominant transporting nuclide may be inferred. Nuclide distributions determined during postirradiation examination can be used to develop models of the transport mechanism.

MASS CHAINS OF PRIMARY INTEREST

The mass chains of primary interest are those having

1. Volatile halogen primary fission fragments and noble gas daughters.

2. Noble gas chain members with relatively long half-lives.

3. Volatile alkali metal chain members with long half-lives.

4. High fission yields.

Inspection of the yield curves and decay chains of Katcoff[5] or Crocker[6] (Figs. 1 through 3) shows that the mass chains of primary interest (i.e., those in the heavy mass region of the fission yield spectrum) result in large fission yields of long-lived or stable cesium, which can interact with mixed oxide fuel, UO_2 axial blanket material, and fission product trap charcoal. The mass chains ending in important cesium nuclides are the 133, 135, and 137 chains; other chains in this mass region result in stable xenon.

In the low mass region, the chains from masses 85 to 93 produce smaller quantities of the volatile alkali metal rubidium. Although fission yields in this region are roughly comparable to those in the heavy mass region, the rubidium metal half-lives are generally short except for the mass 85 and 87 chains. Thus, most transport investigations have been

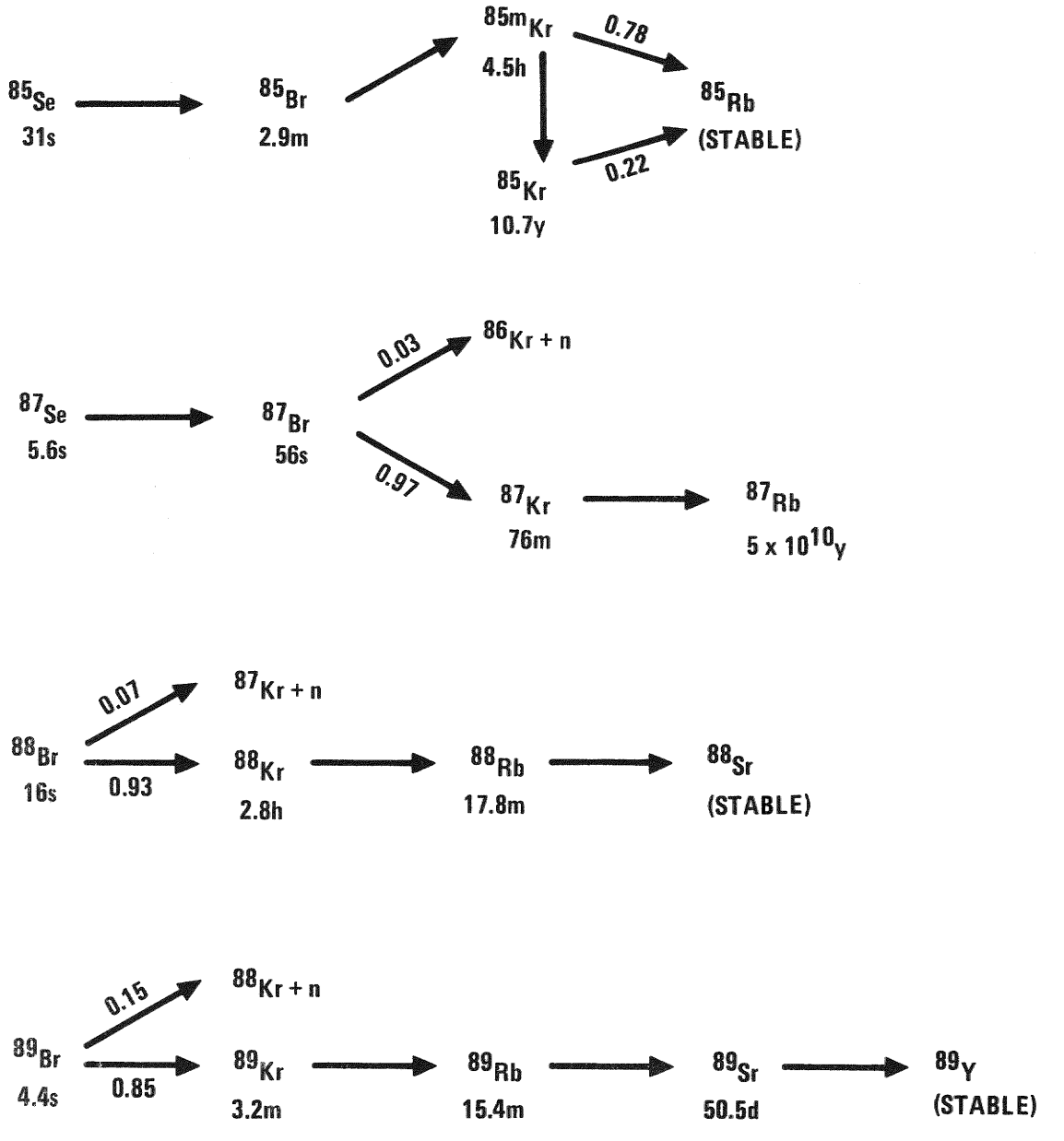

Fig. 1. Fission product decay chains for isotopic masses 85 through 89

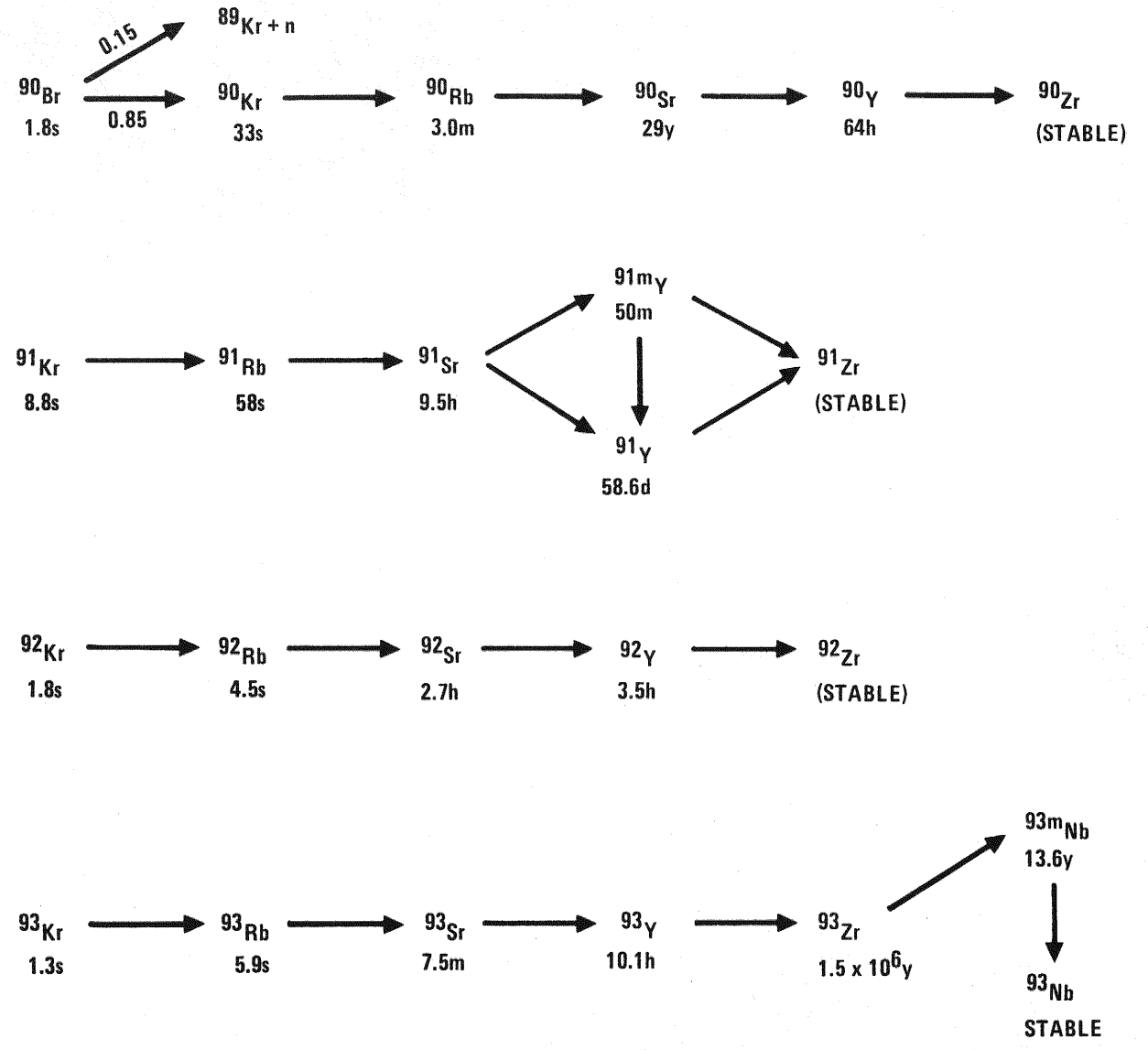

Fig. 2. Fission product decay chains for isotopic masses 90 through 93

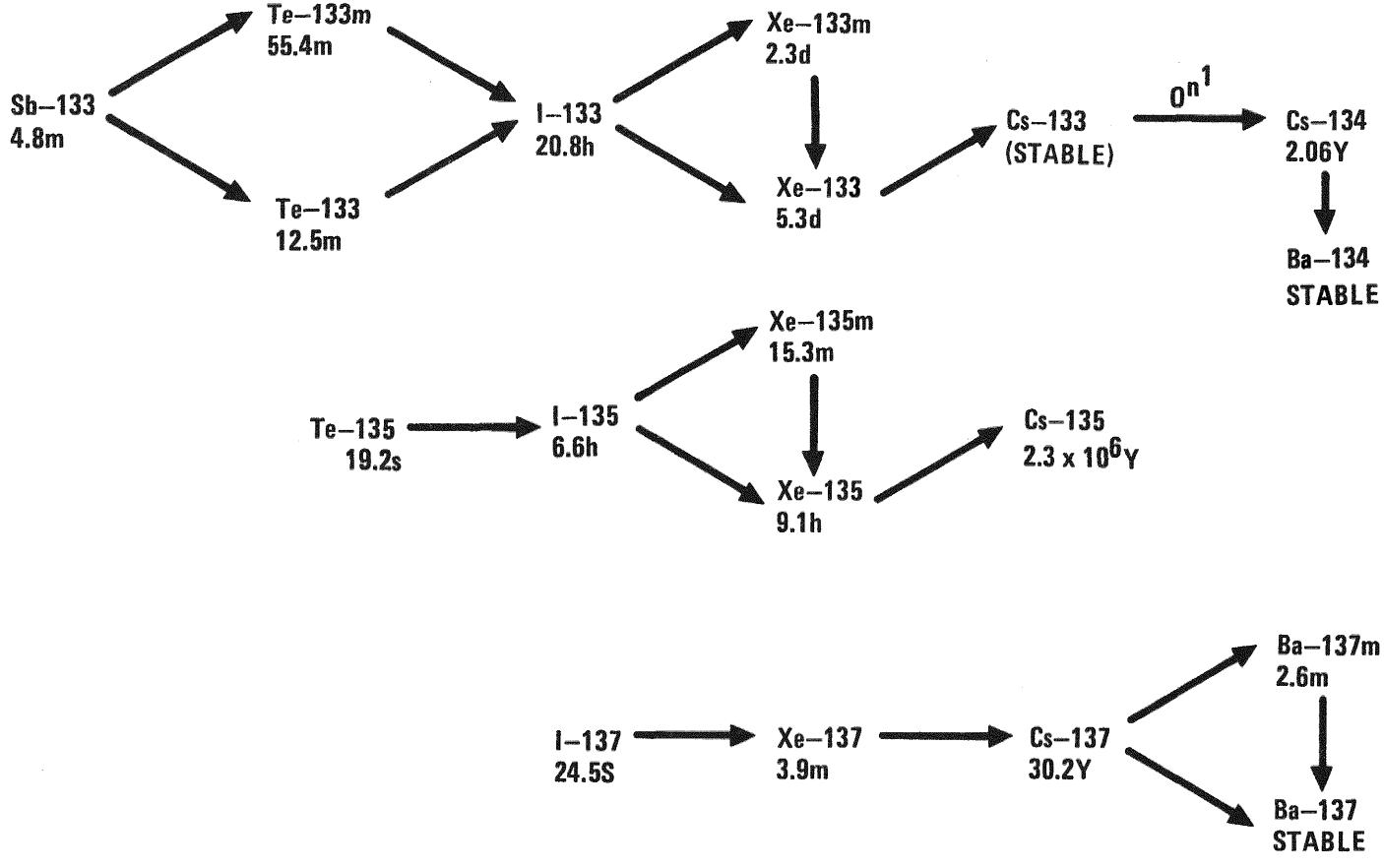

Fig. 3. Fission product decay chains for isotopic masses 133, 135, and 137

directed at the heavy mass region, although this is undoubtedly related to the fact that cesium and xenon are easier to detect than their rubidium and krypton counterparts.

The half-lives of I-133 and I-135 are sufficiently long to be contributors to fission product transport; I-137, on the other hand, is quite short-lived and probably contributes only marginally to transport of the mass 137 chain. The noble gas daughters of the 133 and 135 mass chains and the cesium nuclides resulting from all three mass chains are long-lived and can therefore contribute to chain transport. Cs-137 has been used as a convenient monitor of cesium isotopes because of its hard gamma emission (0.662 MeV) and because Cs-133 and Cs-135 are not detectable by gamma spectroscopy. The data in this paper show that reliance on Cs-137 as an overall cesium monitor is misguided. Cs-134, which is not a fission product, is a better monitor of both Cs-133 and Cs-135 (which together constitute two-thirds of the total cesium). Cs-134 is a neutron activation product from the fission product Cs-133;* it thus monitors the behavior of Cs-133.

Tables I and II give the expected nuclide yields for a simulated GCFR fuel rod (F-1 or F-5 series) irradiated in EBR-II to 100 MWd/kg burnup. These tables indicate potential fuel rod problems that may be attributed to the generation of halogens and alkali metal fission products in significant quantities. In cases where the half-life of the volatile alkali metal is short compared with the reactor residence time, the alkali metal may be found during postirradiation examination as the daughter alkaline earth metal, but the transport processes are most likely to involve the volatile alkali metal or the precursor noble gas. An analogous situation may occur with short-lived halogens, except that long-lived or stable noble gases or daughter alkali metals may be the existing species determined during postirradiation examination. Over 2 g of alkali metals and halogens are available for redistribution from the 34.3-cm fuel columns of EBR-II.

---

*Xe-134 is a stable fission product and undergoes 100% equilibrium release from the fuel; thus, released Xe-134 should be totally vented from the rod.

TABLE I
ALKALI METAL PRODUCTION IN AN F-1 EXPERIMENTAL ROD AT 100 MWD/KG BURNUP

Rubidium				Cesium			
Nuclide	$T_{1/2}$	Fission Yield (%)	Inventory at 100 MWd/kg in EBR-II[a] (mg)	Nuclide	$T_{1/2}$	Fission Yield (%)	Inventory at 100 MWd/kg in EBR-II[a] (mg)
Rb-85	Stable	1.2	41	Cs-133	Stable	6.7	362
Rb-87	5×10^{10} yr	2.2	77	Cs-135	2.6×10^{6} yr	6.6	362
Rb-88	17.8 min	3.1	110 Sr-88	Cs-137	30 yr	6.3	351
Rb-89	15.4 min	4.0	36.4 Sr-89	Cs-138	32.2 min	6.5	362 Ba-138
Rb-90	2.7 min	4.8	175 Sr-90	Cs-139	9.5 min	6.2	(0.16) Ba-139
Rb-91	72 s	5.0	(0.37) Sr-91	Cs-140	66 s	6.0	(35) Ba-140
Rb-92	5.3 s	5.2	(0.11) Sr-92				
Total Rb + Sr			440	Total Cs + Ba			1472

Total alkali and alkaline earth metals = 1912 mg

[a] The inventory values are for stable or long-lived alkali metals (or their alkaline earth daughters as shown). Values in parentheses are steady-state inventories of short-lived alkaline earth metals.

TABLE II
HALOGEN PRODUCTION IN AN F-1 EXPERIMENTAL ROD AT 100 MWD/KG BURNUP

Bromine				Iodine			
Nuclide	$T_{1/2}$	Fission Yield (%)	Inventory at 100 MWd/kg in EBR-II[a] (mg)	Nuclide	$T_{1/2}$	Fission Yield (%)	Inventory at 100 MWd/kg in EBR-II[a] (mg)
Br-79	Stable	0.098	3.15	I-127	Stable	0.32	16.8
Br-81	Stable	0.25	8.4	I-129	1.7×10^7 yr	1.1	57.8
Br-83	2.4 hr	0.52	17.6 Kr-83	I-131	8.05 days	3.3	178
Br-84	31.8 min	0.91	31.3 Kr-84	I-132	2.3 hr	4.7	253 Xe-132
Total Br			11.5	I-133	20.8 hr	6.7	(1.06)
				I-134	52.5 min	7.5	403 Xe-134
				I-135	6.7 hr	6.6	(0.33)
				Total I			252

Total halogen = 264 mg

[a] The inventory values are for stable or long-lived halogens (or the noble gas daughter as shown). Values in parentheses are steady-state inventories of short-lived halogens.

FISSION PRODUCT TRANSPORT PHENOMENA

This section discusses the different conditions present in vented and sealed fuel rod irradiations. These operating conditions determine the fission product transport measurements which can be made during irradiation of vented fuel rods and affect the fission product distribution found in vented and sealed rods during postirradiation examination.

Transport Phenomena in Vented Fuel Rods

The purposes of vented fuel rod irradiations are

1. To confirm the expected performance of vented and pressure-equalized fuel.

2. To determine the release fractions, or R/B,* of fission gas nuclides from the fuel matrix.

3. To determine the venting fractions, or V/B,** of fission gas nuclides from the fuel rod.

4. To confirm the efficacy of the fission product charcoal trap and the axial blanket region in delaying the rate at which fission gas nuclides are vented from the fuel rod.

The experiments were performed under conditions which simulated those in a vented GCFR fuel rod. The GB-9 and GB-10 irradiation experiments

---

*R/B is the ratio of the release rate of a given nuclide from the fuel matrix to its birth rate in fission. It is the instantaneous value of the (integrated) fractional release.

**V/B is the ratio of the venting rate of a given nuclide from the fuel rod to its birth rate in fission.

operated with the fuel under a static helium pressure of 6.8 MPa.* Therefore, within these vented rods the transport of volatile and noble gas fission products released from the fuel matrix was governed by the gas phase interdiffusion of each nuclide into high-pressure helium and by sorption in the charcoal trap. Interdiffusion coefficients at 6.8 MPa and 700°C are typically $\sim 6.4 \times 10^{-2}$ cm^2/s compared with ~ 0.65 cm^2/s at 298 K and 0.1 MPa (i.e., diffusion times are 10 times longer than those at room temperature and pressure). In the fuel region, axial thermal gradients impart an added thermal diffusive force which is not present in the blanket region or the charcoal trap, where the temperature is relatively constant. Interdiffusion imposes a major delay in the transport in the blanket region because the small annular cross section between the blanket pellets and the cladding is essentially the only area available for diffusion. The increased transport times arising from the slow interdiffusion process are unimportant for stable and long-lived fission gases, but they result in markedly decreased transport fractions for radioactive gases whose transport times are significant fractions of their half-lives. Decay of the diffusing noble gases to cesium daughters can occur as a consequence of these delay times, resulting in plateout in the blanket region or the charcoal trap. Both locations present surfaces on which the cesium is tightly bound: in the blanket region as Cs_2UO_4 and in the charcoal trap as chemisorbed cesium. Further movement from either region is unlikely since temperatures are much less than 800°C. Thus, in vented fuel rods, long-lived and stable fission gases should be vented from the rod at essentially the same fraction as those released from the fuel; i.e., V/B $\sim$ R/B. Short-lived noble gases, on the other hand, are expected to decay to volatile cesium (or rubidium) daughters in the blanket region or the charcoal trap and should be permanently retained in these locations. Generally, the movement of volatile fission products in vented fuel rods cannot be measured during operation, although some data on the contribution of iodine to the transport of the 133 and 135 mass chains can be obtained by special

*To simulate the GCFR condition of essentially zero stress on the cladding, the static NaK heat transfer fluid between the fuel rod and the experiment capsule was operated with 6.6 MPa of helium as a cover gas.

procedures. Results of fission product release and transport measurements in vented fuel rods are given in the following section.

Transport Phenomena in Sealed Fuel Rods

In sealed fuel rod irradiations such as the GCFR F-1 and F-5 series [and in liquid metal fast breeder reactor (LMFBR) irradiations], all fission products (with the probable exception of tritium) are retained within unfailed rods. Unlike vented fuel experiments, in which the bulk of the data is obtained during irradiation, no information on fission product transport can be obtained for sealed fuel during reactor irradiation. However, data on fission product distributions within the rod can be obtained during interim and postirradiation examinations. The transport processes which contribute to fission product migration in the rod can be inferred from these distribution data.

Unlike vented rods, in which the internal gas pressure is high (8.6 MPa) and constant throughout irradiation, the initial helium gas pressure in sealed fuel rods is 0.3 MPa (at operating temperature). The internal gas pressure rises essentially linearly with burnup to ∿3 MPa (∿450 psi at 5 at. % burnup) as stable and long-lived xenon and krypton are produced by fission. Long-lived fission gases will pressure equilibrate throughout the rod, and the gases will sorb on the charcoal, with higher concentrations at lower temperatures. Decay to alkali metal daughters will then result in essentially permanent retention of the metal. Short-lived noble gases must migrate from the hot fuel region through the narrow blanket pellet-cladding gap by gas phase interdiffusion. As the internal pressure rises to ∿3 MPa, the interdiffusion coefficient decreases by one order of magnitude, and transport delay times in the blanket region can exceed several half-lives for short-lived species. The migration of short-lived noble gases beyond the blanket region is thus markedly impeded, and steep gradients in cesium daughter concentrations may be expected in either the blanket region or the charcoal trap.

A major objective during postirradiation examination of sealed fuel rods is to determine, if possible, whether volatile fission nuclides are responsible for any significant fraction of the transport process beyond the blanket region. It is clear from many observations[7-10] that volatile species are responsible for transport to the fuel-blanket interface, as evidenced by the large Cs-137, Cs-134, and I-131 peaks found by gamma spectrometry at the fuel-blanket interface. (Some of these data are presented in the following section.) There is even some evidence that the iodine precursor Te-132 may be a volatile transporting nuclide in fast breeder reactor irradiations.[7] Therefore, in sealed fuel rods, significant quantities of alkali metals are expected in the charcoal because of

1. The containment of all noble fission gases within the sealed rod.

2. The low temperature (350° to 500°C) of the charcoal and its sorption of noble gases.

3. The high retentivity of charcoal for the daughter alkali metals at temperatures below ~1000°C.

RESULTS AND DISCUSSION

This section discusses the measurements of noble gas transport and release in vented rod irradiations GB-9 and GB-10. The fission product distributions in the F-1 series of sealed rods determined during post-irradiation examination are also presented. These data are utilized to infer the predominant transport processes for each mass chain.

Vented Rod Irradiations

GCFR vented rod experiments GB-9 and GB-10 were irradiated in the Oak Ridge Research Reactor (ORR) as a cooperative effort of General Atomic (GA), Oak Ridge National Laboratory (ORNL), and Argonne National Laboratory

(ANL). Previous publications[11,12] have described the design and operation of these vented fuel rod experiments. This paper discusses only the results pertinent to fission product transport mechanisms.

Fission gas release and venting rates were measured from GCFR vented fuel rods irradiated in capsules GB-9 and GB-10. The release rate R is the rate at which gaseous fission products born in fission of the fuel are released from the solid-state matrix of the mixed oxide fuel into the gas phase of the fuel region interstices. The venting rate V is the rate at which the gaseous fission products are released and then transported in the gas phase from the fuel region through the blanket and trap regions to the fuel rod vent. Dividing the release and venting rates by the birth rate B results in R/B and V/B, the release* and venting fractions, respectively. At low pressure there is little distinction between the release and venting fractions, but in the GCFR with high-pressure helium (8.6 MPa) in the fuel rod and in experiments GB-9 and GB-10 (6.8 MPa), there is much greater impedance to the gas-phase transport, which results in significant differences in the R/B and V/B values.

The design of the sweep gas lines of capsule GB-9 enabled only V/B to be measured; these data have been reported[11]. The R/B values for the gaseous nuclides calculated from the V/B values and theoretical values for the venting-to-release rates V/R were not satisfactory, and direct measurement of R/B values was deemed necessary. The greatly increased capabilities of the GB-10 sweep gas system permitted, for the first time, direct measurement of fission gas release from an operating simulated fast breeder reactor fuel rod. Good fission gas release data were acquired at three power levels and cladding outer surface temperatures [39 kW/m (565°C), 44 kW/m (620°C), and 49 kW/m (685°C)] by sweeping gas directly through the fuel region when measuring R/B and conducting it to the sampling or measuring points. Typical data are given in Table III.[12] Early measurements used "grab gas samples," as in the GB-9 V/B

*The integral of R/B over time is the fractional release.

TABLE III
FISSION GAS RELEASE FRACTIONS (R/B) MEASURED IN CAPSULE GB-10 AT VARIOUS BURNUPS, POWER LEVELS, AND CLADDING TEMPERATURE LEVELS[a]

Isotope	Half-Life	R/B[b] (%)					
		39 kW/m			44 kW/m		
		6.8 MWd/kg	14.6 MWd/kg	23.9 MWd/kg	27.9 MWd/kg	35.6 MWd/kg	58.5 MWd/kg
Kr-85m	4.4 hr	1.1	2.1	1.6	11.0	5.9	5.2
Kr-87	1.3 hr	0.35	0.43	0.95	7.0	3.7	3.0
Kr-88	2.8 hr	0.38	0.49	1.1	4.8	3.0	2.8
Kr-89	3.2 min	--	--	0.22	2.2	0.85	1.0
Xe-133m	2.3 days	--	--	--	15.0	13.0	--
Xe-133	5.3 days	5.2	5.2	6.2	15.0	13.0	2.9
Xe-135m	15 min	0.52	0.70	1.3	5.2	3.0	2.5
Xe-135	9.2 hr	1.3	2.1	2.7	11.0	6.0	5.5
Xe-138	17 min	0.28	0.52	0.63	3.7	1.8	1.8

[a] From Ref. 12.

[b] R/B data acquired at 49 kW/m and 685°C between burnups of ∿75 and 104 MWd/kg have not been processed.

measurements. Later GB-10 R/B and V/B measurements were performed using an on-line Ge(Li) gamma spectrometer mounted in the effluent sweep gas line.

Figure 4 presents typical R/B and V/B data as a function of burnup for Xe-133 and Xe-135m, the longest- and shortest-lived fission products of interest. The effects of changes in power levels, temperatures, and capsule gas pressure are also apparent in Fig. 4. When the power level was changed from 39 to 44 kW/m, the transient caused overshooting of R/B as a consequence of release of the fission gas stored in the fuel matrix at the lower power level. The R/B for Xe-133 exceeded a value of 1.0 for a short time.

The effect of variation of helium gas pressure on R/B and V/B is also apparent in Fig. 4. As the pressure is reduced, R/B and V/B increase; as pressure is increased, R/B and V/B decrease. R/B and V/B vary in a transient manner and reach steady-state values at each pressure level. The effects of gas pressure on V/B and V/R, which depend on gas-phase diffusion, were anticipated. However, gas pressure also affects R/B, which is primarily dependent on the solid-state diffusion, or migration, process. Again, the effect is transient. However, the data do not permit extraction of quantitative results, but indicate an area where future research may be fruitful.

Over the range of half-lives for which data were collected, R/B is approximately proportional to the square root of half-life. Since such dependence is usually indicative of a diffusion-controlled process, the data have been treated assuming such a model. The solid-state diffusion parameters for the spherical particle model of fission gas release[13] have been modified using the GB-10 release data. In the equation $D = D_o e^{-Q/kT}$ (where D is the diffusion parameter in cm^2/s, Q is the activation energy in eV, k is the Boltzmann constant, and T is the absolute temperature in K), the base diffusion parameters D_o which best fit the GB-10 data were found to be 1.21×10^{-10} and 7.52×10^{-10} cm^2/s for krypton and xenon isotopes,

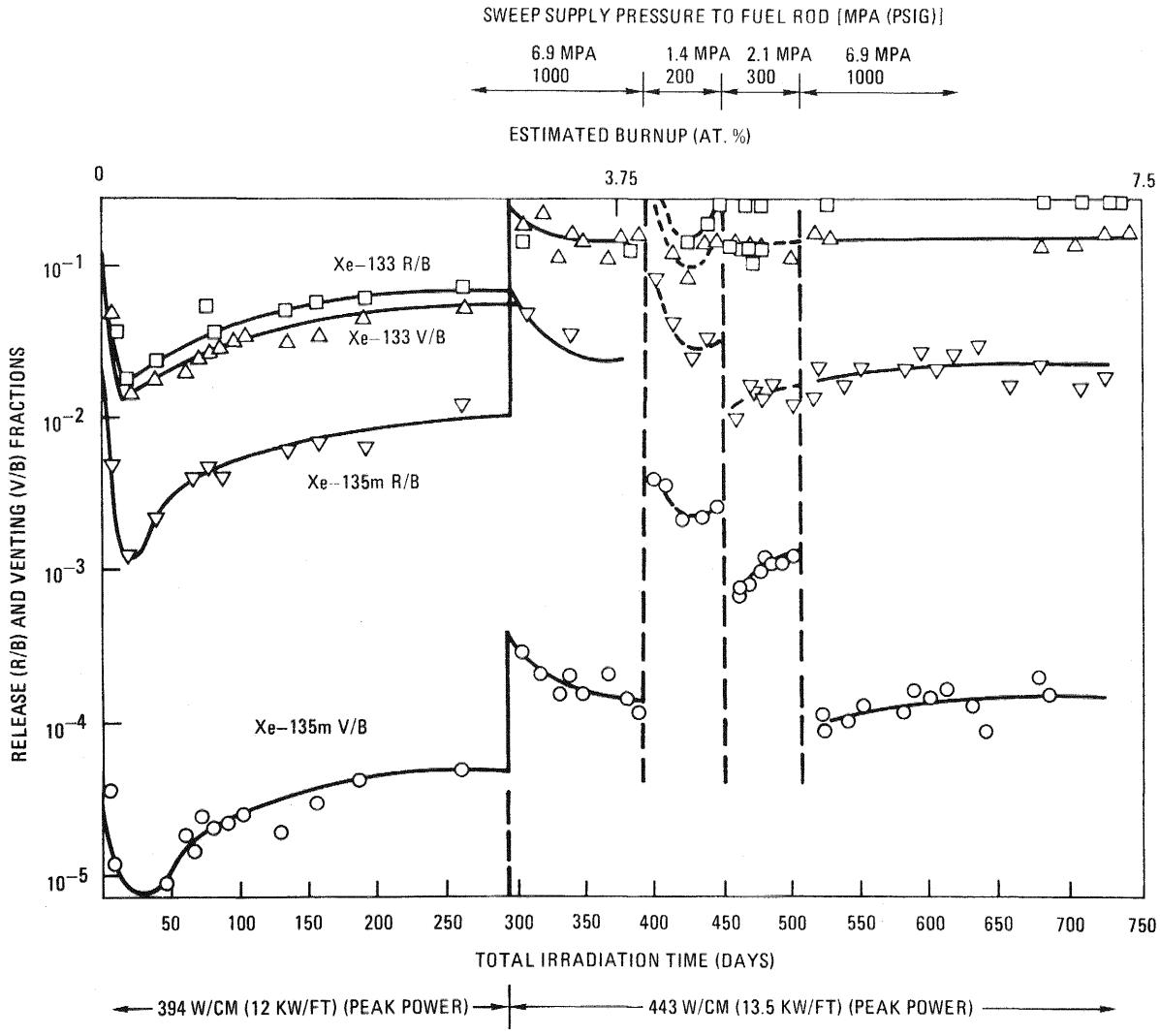

Fig. 4. GCFR capsule GB-10 release (R/B) and venting (V/B) fractions

respectively, when activation energies of 1.62 and 1.89 eV (previously determined by Findlay et al.[14]) were used. The revised diffusion parameters are factors of about 22 and 12 less, respectively, than the diffusion parameters of Findlay et al. determined under isothermal conditions to burnups of 50 MWd/kg.

To adjust the diffusion parameters for the GB-10 data, the temperature distribution in the GB-10 fuel rod was calculated from measured power and cladding temperatures using the LIFE-III code.[15] The spherical particle model release equations were then applied to incremental fuel volumes at their calculated temperatures to obtain differential volume releases. In turn, the releases were summed to give the total release, and the diffusion parameters were adjusted to give the best fit of calculated to measured releases for all krypton and xenon isotopes. Additional postirradiation examination data must still be correlated with the calculated fuel temperatures before the diffusion parameter values can be firmly established and their accuracy assessed. (Correlation of the diffusion parameters and activation energies for krypton and xenon with the GB-10 data is the subject of a separate paper at this conference.[16]

Figure 5 shows R/B as a function of half-life. The slope of the R/B versus $T_{1/2}$ curve is approximately proportional to $\sqrt{T_{1/2}}$. In contrast, the analogous plot of V/B versus $T_{1/2}$ in Fig. 6 shows a steeper slope, which is approximately proportional to $T_{1/2}$ for both xenon and krypton nuclides. It is clear, however, that as the half-lives become very short, the slope becomes steeper, since decay occurs so rapidly that significant nuclide migration cannot occur. At the other end of the spectrum, R/B and V/B must approach unity for stable isotopes. Unfortunately, the data on the stable fission gases from the GB-10 experiment were not of adequate quality to confirm this expected behavior. However, analysis of the fission gas mixture removed from the plena of the F-1 experiment sealed rods showed that ∿73% of the stable xenon species and ∿81% of the stable krypton nuclides were released from the fuel matrix.

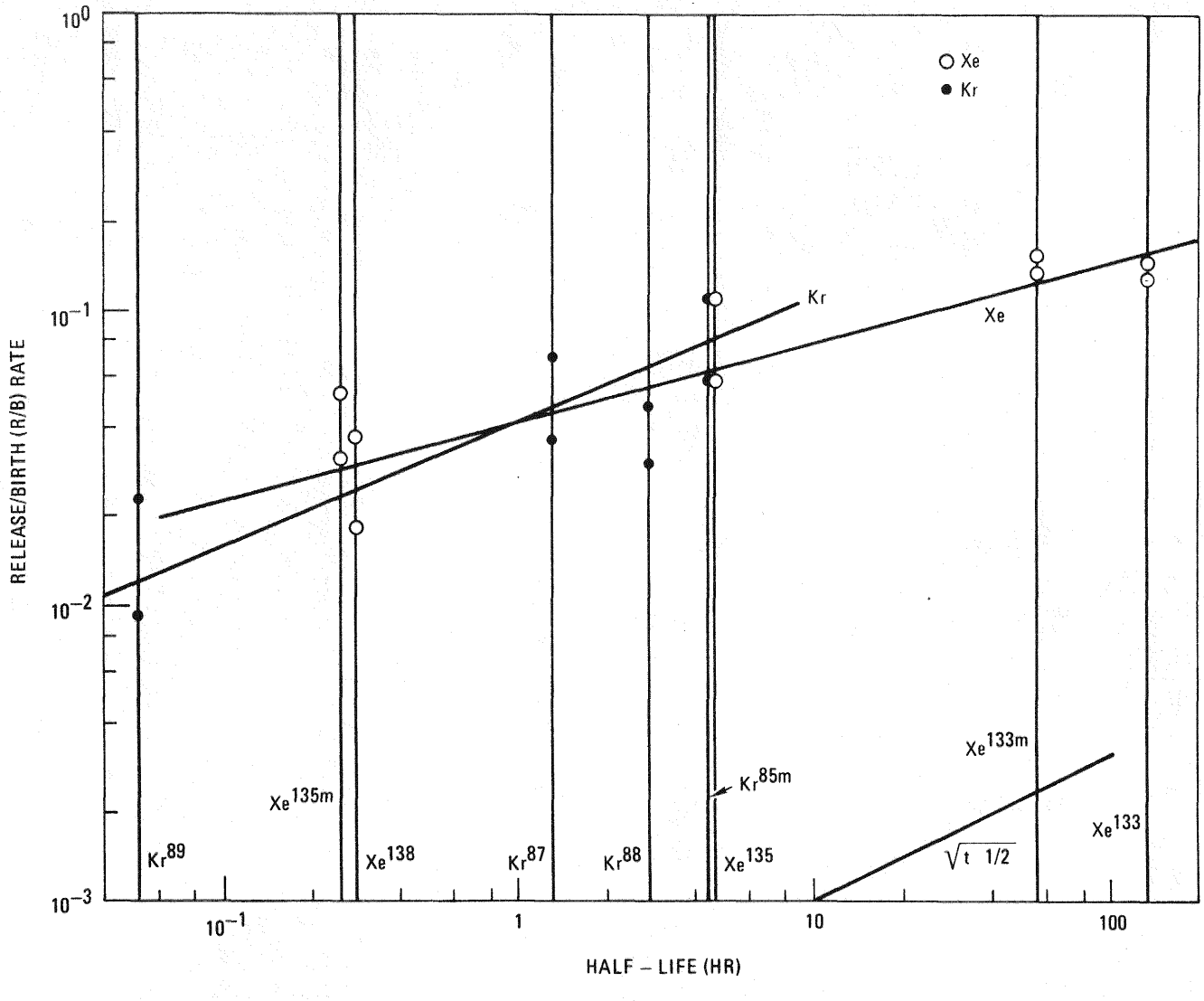

Fig. 5. Fission gas isotope release fraction (R/B) versus half-life (GB-10 experiment)

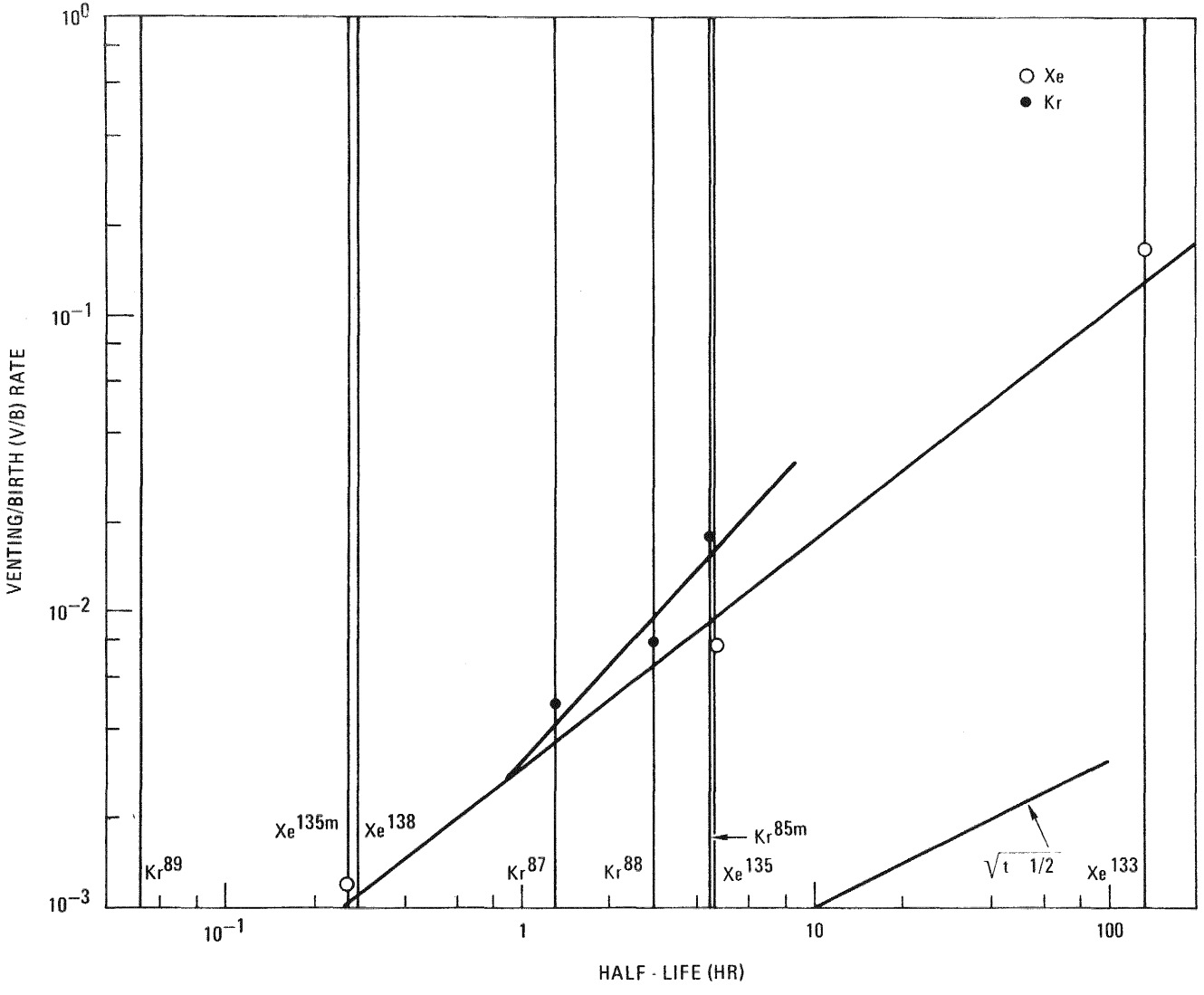

Fig. 6. Fission gas isotope venting fraction (V/B) versus half-life (GB-10 experiment)

A special series of measurements carried out during the GB-10 experiment demonstrated that the xenon gas and its iodine precursor were released from the fuel matrix and jointly contributed to the measured V/B for the 133 and 135 mass chains. These data were acquired by determining the total V/B for each mass chain while the capsule was operating at power and then continuing the V/B measurements as a function of time after scramming the reactor. Upon scram, no more xenon or iodine was born from fission; however, iodine born and released from the fuel during reactor operation continued to decay to xenon, which was then found in the vented gas. The difference between the V/B observed during operation at power and that observed during shutdown is the fraction of the mass chain released from the fuel as xenon. These data are given in Table IV for the 133 and 135 mass chains[11].

Since the R/B values for the 133 and 135 mass chains are about 6.2% and 22.%, respectively, at 37.4 kW/m, I-133 accounts for ∿40% of the total release of the 133 mass chain, and I-135 for ∿50% of the total release of the 135 mass chain. The corresponding fractions for the 48.6-kW/m power level cannot be determined until R/B data for the noble gases have been analyzed at that power level. However, the data indicate that only a small fraction of the iodine released from the fuel matrix reaches the charcoal trap. Most of that released from the fuel therefore plates out in the blanket region. Longest and Conlin[12] report that during normal capsule operation the charcoal trap contains only a 1.2×10^{-4} fraction of the I-135 inventory and a 2.2×10^{-4} fraction of the I-133 inventory. These results are in reasonable agreement with results of Langer, Buzzelli, and Flynn,[17] who found only a 2.3×10^{-5} fraction of the stable iodine species I-127 and a 4.3×10^{-5} fraction of long-lived I-129 in the charcoal trap of the GB-9 experiment. Iodine inventories for the GB-10 charcoal trap are not yet available.

In contrast to the small transport of iodine to the charcoal trap in both the GB-9 and GB-10 experiments, significant quantities of the longer-lived cesium nuclides were found in the charcoal trap of the GB-9 experiment. These data are given in Table V[17].

TABLE IV
RELEASE FRACTIONS FOR IODINE NUCLIDES FROM GB-10 FUEL

Linear Rod Power (kW/m)	R/B	
	I-133	I-135
37.4	2.5×10^{-2}	1.5×10^{-2}
48.6	1×10^{-1}	3.5×10^{-1}

TABLE V
FRACTIONAL INVENTORY OF CESIUM ISOTOPES
IN THE CHARCOAL TRAP OF CAPSULE GB-9

Nuclide	Half-Life (yr)	Half-Life of Xenon Precursor	Fractional Inventory in Trap
Cs-133[a]	Stable	5.3 days	1.5×10^{-3}
Cs-135	2×10^{6}	5.8 h[b]	1.9×10^{-3}
Cs-137	30	3.9 min	3.9×10^{-5}
Total cesium			1.1×10^{-3}

[a] Includes Cs-134 derived from 133 mass chain.

[b] Effective half-life of Xe-135 in the Oak Ridge reactor; the natural half-life is 9.2 h.

Since the half-lives of all the cesium nuclides are long compared with the transport time, the difference between the 137 chain transport and the transport of the 133 and 135 chains cannot be ascribed to the cesium chain members. On the other hand, the 133 and 135 xenon precursors are relatively long-lived, but Xe-137 has a 3.9-m half-life. Thus, these data indicate that the transport of the xenon precursor primarily determines the fraction of the mass chain transported to the charcoal trap. Unfortunately, isotopic inventories for the upper blanket region of the GB-9 fuel rod were not obtained, so this hypothesis could not be tested.

Sealed Rod Irradiations

In sealed GCFR irradiation experiment F-1 (X094), 13 rods containing mixed oxide fuel, axial UO_2 blankets, and charcoal traps at each end of the rod were irradiated to burnups of 2.5 to 13.6 at. %. The characteristics of these rods are given in Table VI. Details of the F-1 (X094) fast flux irradiation experiment are presented in two companion papers at this conference[4,18]. The discussion in this paper is limited to the fission product distributions in the F-1 rods determined during postirradiation examination and the implications of these distributions for the transport processes in the sealed rods.

Postirradiation examination of the rods included axial gamma spectrometric analysis to determine overall fission product distributions and to guide destructive postirradiation examination. The axial gamma spectrometry profiles for rods G-4, G-8 (no charcoal trap), G-9, and G-13 are shown in Figs. 7 through 10. These data were analyzed by Langer and Buzzelli[19] to provide semiquantitative measurements of cesium isotope distributions in the fuel rods irradiated to burnups of 8.9 to 13.6 at. %. The data also demonstrated isotopic fractionation of cesium in the fuel rods, which occurs as a consequence of the different predominant mode of transport of the 137 mass chain contrasted to the 133 and 135 mass chains. The data from six of the seven rods of the last sequential loading of

TABLE VI
IRRADIATION CONDITIONS FOR F-1 (X094) FAST FLUX IRRADIATION EXPERIMENT FUEL RODS

Fuel Rod Identification No.	Fuel O/M	Cladding I.D. Temperature (°C)	Linear Rating (W/cm)	Burnup (at. %)	Calculated Exposure [$n/cm^2 \times 10^{22}$ (E > 0.1 MeV)]	Remarks
G-1	1.992	740	453	5.6	3.4	No charcoal trap
G-2	1.971	730	459	5.3	3.4	No charcoal trap
G-3	1.987	669	430	2.7	1.7	
G-4	1.983	683	456	13.6	6.7	
G-5	1.990	716	462	5.1	3.4	No charcoal trap
G-6	1.972	662	452	4.9	3.4	
G-7	1.984	648	472	4.8	3.4	
G-8	1.985	696	492	10.3	5.6	No charcoal trap
G-9	1.947	706	475	8.9	4.2	
G-10	1.968	722	495	9.8	4.2	
G-11	1.968	731	521	9.6	4.2	
G-12	1.976	714	472	9.7	4.2	
G-13	1.973	759	521	9.5	4.2	

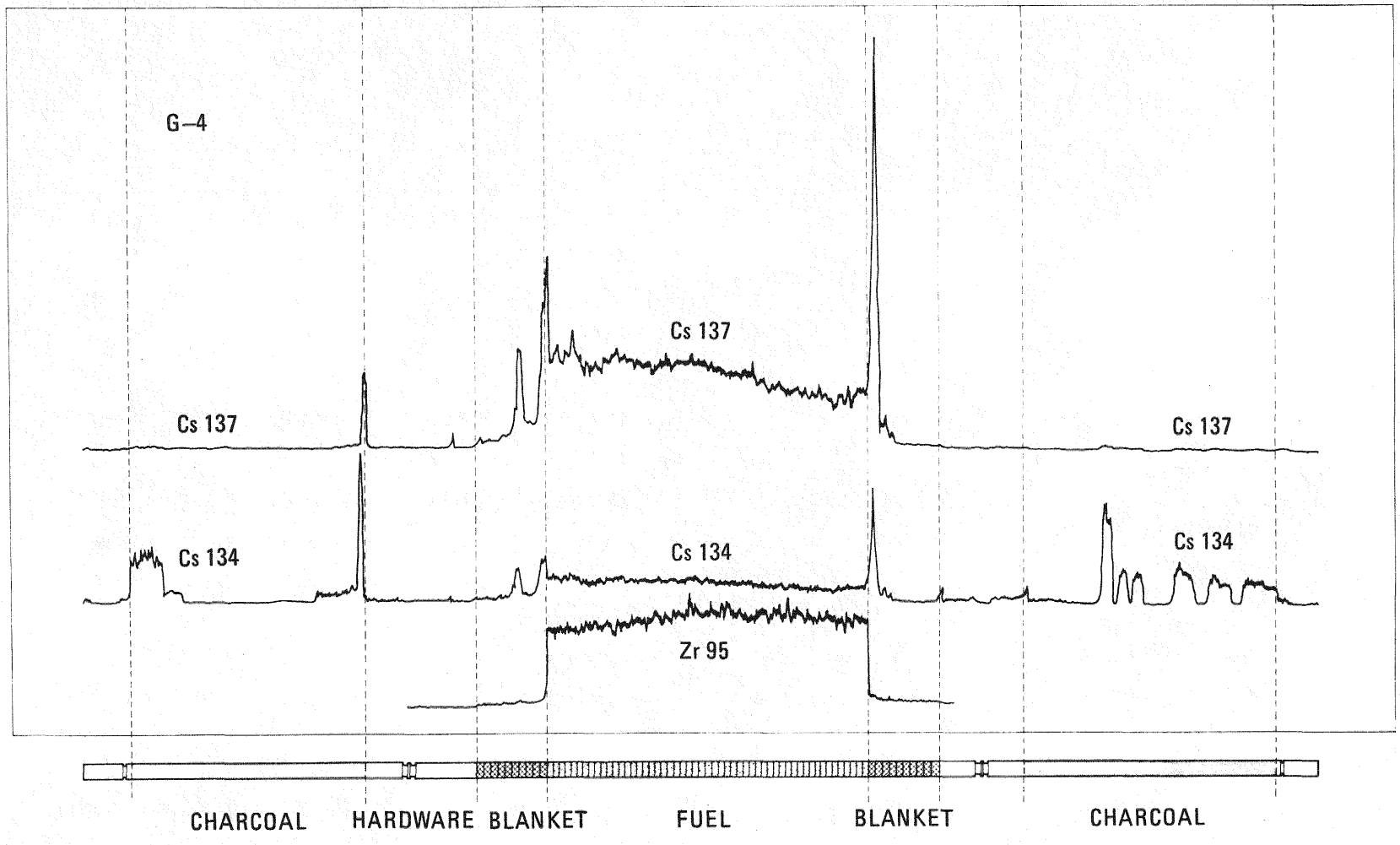

Fig. 7. Axial gamma scan for F-1 fuel rod G-4

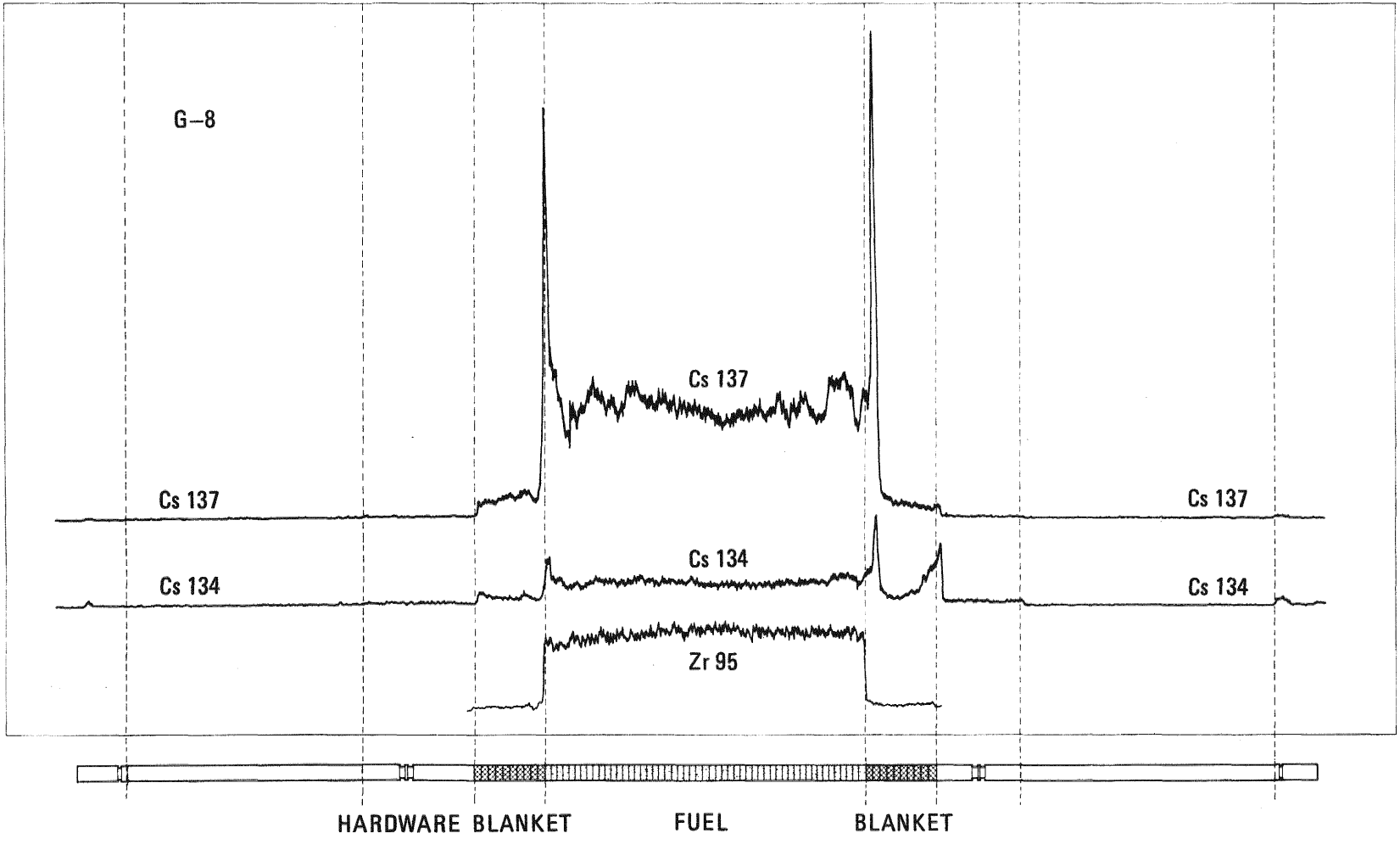

Fig. 8. Axial gamma scan for F-1 fuel rod G-8

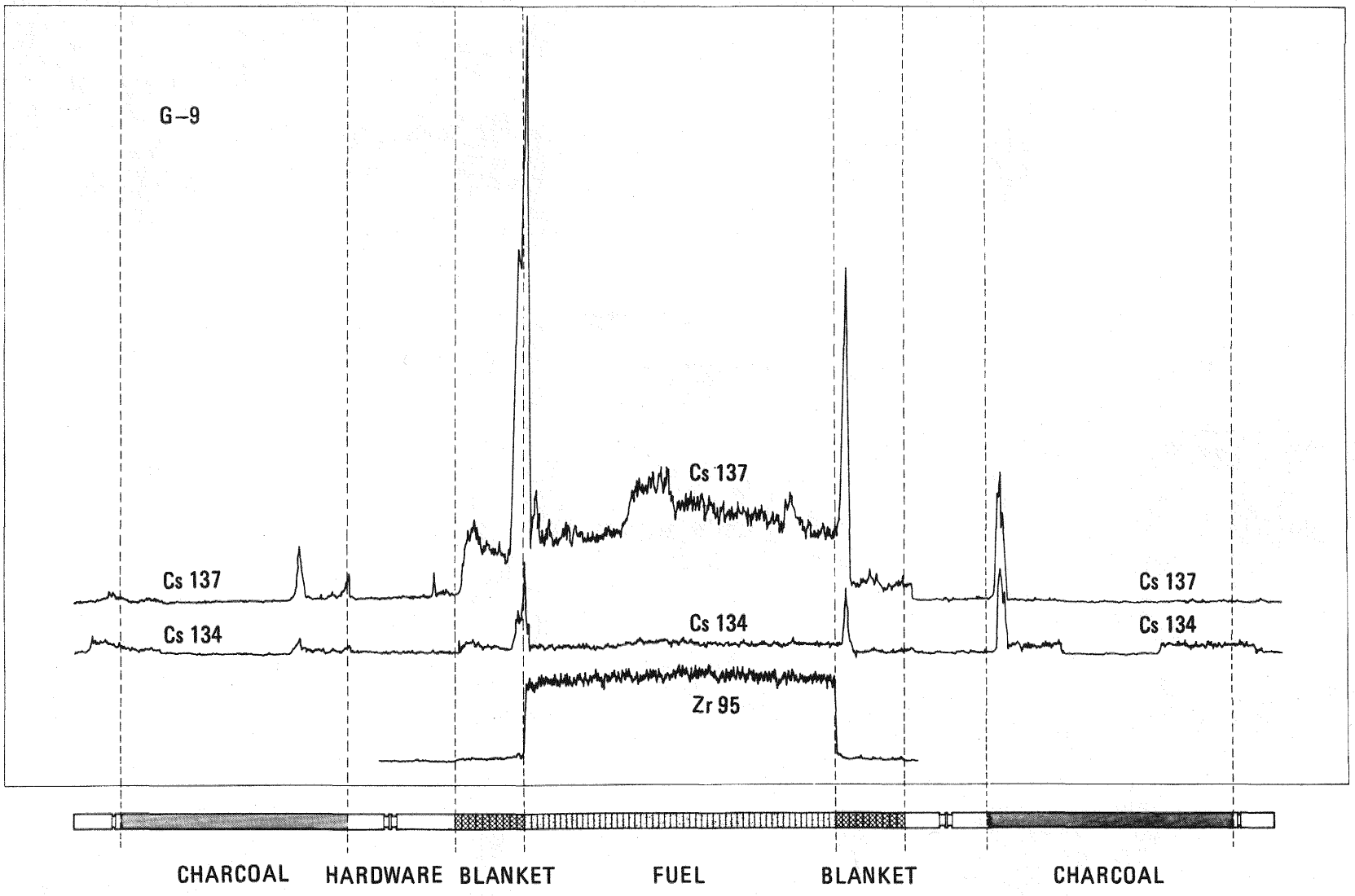

Fig. 9. Axial gamma scan for F-1 fuel rod G-9

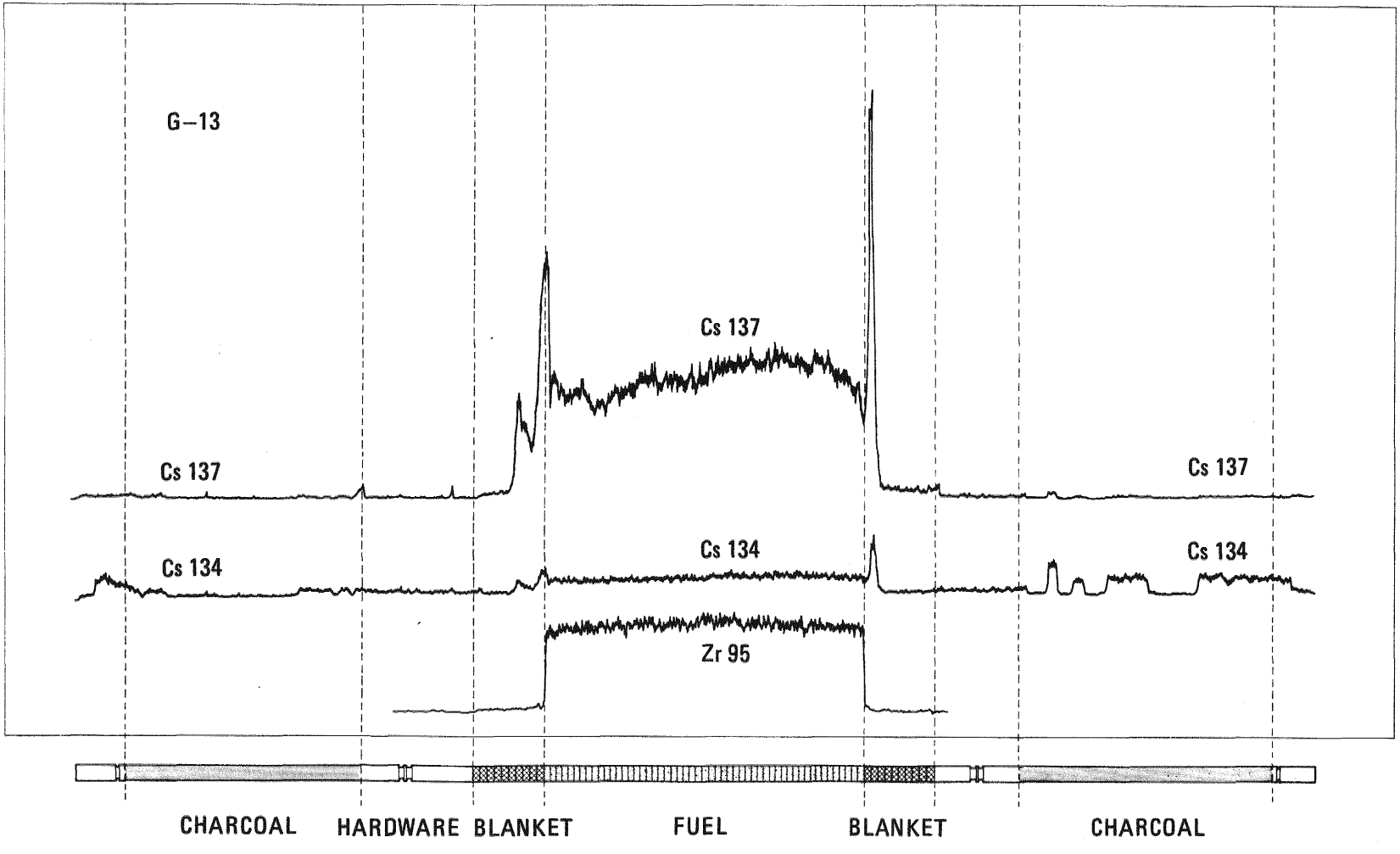

Fig. 10. Axial gamma scan for F-1 fuel rod G-13

the F-1 (X094) experiment are shown in Table VII and demonstrate the following:[19]

1. The majority of the Cs-137 inventory was retained in the fuel region of the F-1 rods. Retention in the fuel region decreased from ∿80% to ∿55% as the cladding temperature was raised from ∿675° to 730°C.

2. Generally, less than half the Cs-133 mass chain (as determined by the Cs-134 monitor) was retained within the fuel region.

3. Cesium-137 retention in the fuel region was promoted by low cladding temperature or high oxygen to metal ratio (O/M) in the fuel. It is not clear which parameter is more important; both cladding temperature and O/M appear to influence retention strongly. (Cladding temperature was principally the consequence of differing thermal barrier thicknesses, since all rods had similar linear power ratings.) Figure 11 shows fuel region retention as a function of O/M. In contrast, Cs-134 retention is apparently not dependent on O/M. This seems logical, since a significant fraction of the 137 chain is released as cesium whose binding energy is certainly O/M dependent; Cs-134 is released primarily as the inert gas Xe-133, which should not be O/M dependent.

4. Cesium-137 deposited predominantly in the axial blanket region with an apparent enhancement of the transport to the upper axial blanket in preference to the lower axial blanket in rods with a low O/M. In rods with a high O/M, the transport to each axial blanket was approximately equal. Plateout of large quantities of Cs-137 at the fuel-blanket interface has been observed by a number of investigators[7-10]. Figures 7 through 10 show the typical large peaks at the fuel-blanket interface due to Cs-137 gamma activity as shown in axial gamma spectrometric scans of

TABLE VII
DISTRIBUTION OF CESIUM ISOTOPES IN F-1 FUEL RODS

Rod No.	Burnup (MWd/kg)	Cladding Temperature (°C)	Linear Power (kW/m)	Fuel O/M	Percentage of Isotope in Each Region [a]				
					Lower Charcoal Trap	Lower Axial Blanket	Fuel Region	Upper Axial Blanket	Upper Charcoal Trap
					Cs-137				
G-4	121	683	45.6	1.98	0.2	10	80	8	1.4
G-8	96	696	48.6	1.99	(b)	8	86	7	(b)
G-9	71	706	48.0	1.95	5	9	54	22	8
G-10	71	722	48.0	1.97	--	14	68	14	4
G-11	71	731	50.4	1.97	2	6	51	38	2
G-13	71	759	50.4	1.97	2	11	60	21	6
					Cs-134 [c]				
G-4	121	683	45.6	1.98	23	5	40	6	17
G-8	96	696	48.6	1.99	(b)	14	67	7	(b)
G-9	71	706	48.0	1.95	27	2	46	5	16
G-10	71	722	48.0	1.97	23	4	42	8	16
G-11	71	731	50.4	1.97	27	8	40	14	12
G-13	71	759	50.4	1.97	22	6	41	6	15

[a] Values are rounded and do not necessarily total 100%, since small fractions of cesium were deposited on metallic components.

[b] This rod did not contain active charcoal traps.

[c] The Cs-133/Cs-134-ratio is higher in the upper trap than in the lower trap (owing to thermal flux suppression by banked control rods in the upper section of the EBR-II core). The apparent increased Cs-134 loading in the lower trap may disappear if a thermal flux correction is applied to the data.

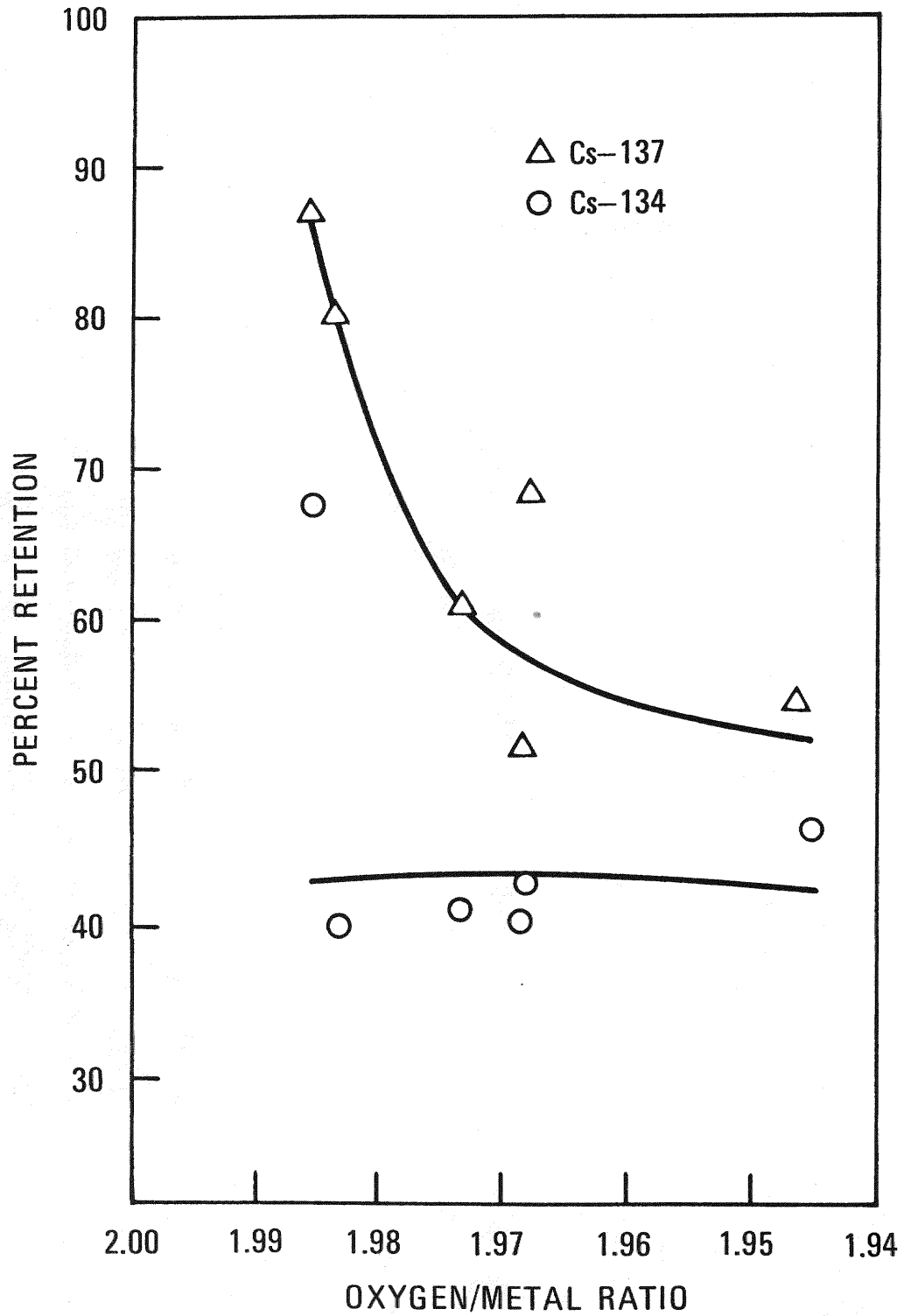

Fig. 11. Cesium retention in fuel region as a function of O/M ratio

fuel rods. The mere existence of the huge maxima in the axial gamma scans is conclusive evidence for vapor phase transport of volatile Cs-137 (or other volatile species, e.g., ^{137}CsI, $^{137}Cs_2O$, $^{137}CsOH$, $^{137}CsBr$) to the interface, where the volatile species plates out as the temperature drops precipitously. Such a profile could not result if transport occurred as the noble gas precursor.

5. Cesium-134, which traces Cs-133, deposited predominantly in the charcoal traps beyond the axial blanket regions. The xenon precursor, which is the primary transporting species, pressure-equilibrated throughout the rod, sorbed on the activated charcoal, and was thus concentrated in the cooler charcoal trap regions. Decay of xenon to cesium will essentially permanently fix the cesium at the decay site in the charcoal trap.

6. Release of cesium from the fuel region may be enhanced by charcoal traps in the fuel rod which lower the cesium chemical potential in the low-temperature portion of the rod and thereby enhance the concentration gradient and promote cesium release.

Since Cs-135 is a long-lived beta emitter, its profile could not be determined by gamma spectrometry. However, the mass chain decay schemes indicate that Cs-135 transport should be qualitatively similar to, but quantitatively different from, that of Cs-133. The iodine precursors of both chains have sufficiently long half-lives so that they can be released from the fuel and contribute to transport at least to the blanket region; the xenon precursors have even longer half-lives and are expected to be the principal contributors to transport to the charcoal trap region of the rod.

Charcoal in the fission product traps of the F-1 experiment rods underwent radiation-induced shrinkage in the fast flux of the EBR-II reactor. Such behavior was not observed in charcoal irradiated in the

thermal flux of the ORR in the GB-9 and GB-10 experiments. Volumetric shrinkage ranging between 45% and 60% occurred for charcoal irradiated in rods which attained burnups up to 13.6 at. %. Approximately 90% of the observed shrinkage occurred in the first 2.5 at. % burnup, as estimated from neutron radiographs taken during interim examinations of the F-1 experiment. Stainless steel screens were used to separate axial sections of the charcoal in the traps and to facilitate separation of the axial sections during postirradiation examination so that fission product concentration profiles in the charcoal trap could be determined. Comparison of the radiograph with detailed axial gamma scans of the trap (Fig. 12) showed that Cs-134 was concentrated in trap regions containing the densified charcoal; Cs-137 did not achieve trap region concentration levels above the in-cell background. If volatile Cs-137 were an important transporting species for this mass chain, detectable levels would have been expected in the charcoal.

Detailed chemical, radiochemical, and mass spectrometric analyses of charcoal samples from axial sections of the traps of several rods were carried out to determine the axial concentration profiles of the fission product nuclides in the traps. It was hoped that these analyses would provide conclusive evidence either for or against the hypothesis of vapor phase transport of Cs-137 to the charcoal trap region of the fuel rod. Figures 13 through 16 show the axial concentration profiles in the traps of rods G-4, G-6, G-9, and G-13 (4.9 to 13.6 at. % burnup). The data, although somewhat scattered owing to sampling errors and counting statistics, indicate the following:

1. The distributions Cs-133, Cs-134, and Cs-135 in the charcoal trap are rather uniform, although there is some apparent enhancement as distance from the core increases. This is perhaps due to the lower trap temperature and hence greater sorption capacity of the charcoal.

2. The concentration of Cs-133 in the traps exceeds that of Cs-135 by a factor of approximately 2. Since the fission yields in the

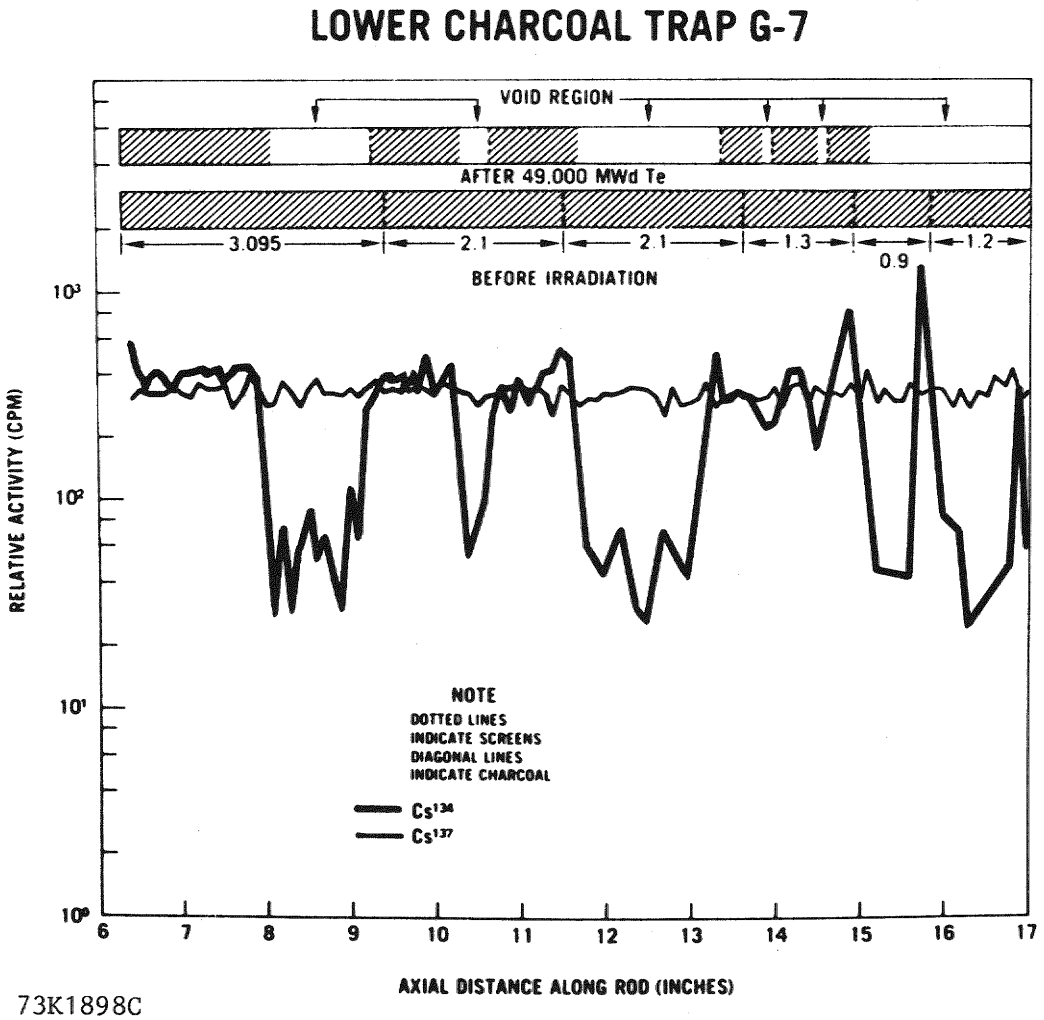

Fig. 12. Comparison of charcoal trap neutron radiograph with trap axial gamma scan

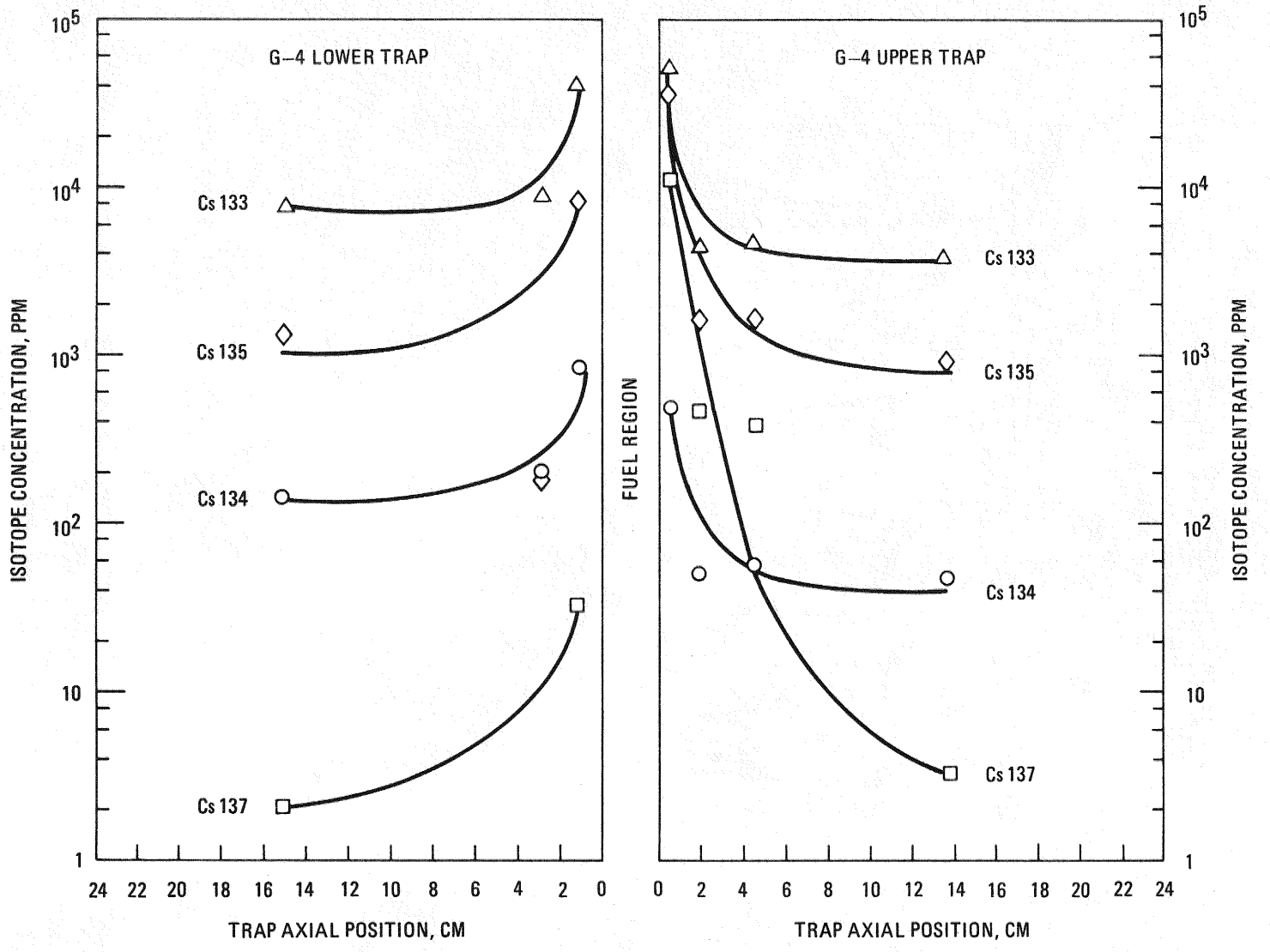

Fig. 13. Axial cesium concentration profiles for F-1 fuel rod G-4 charcoal traps

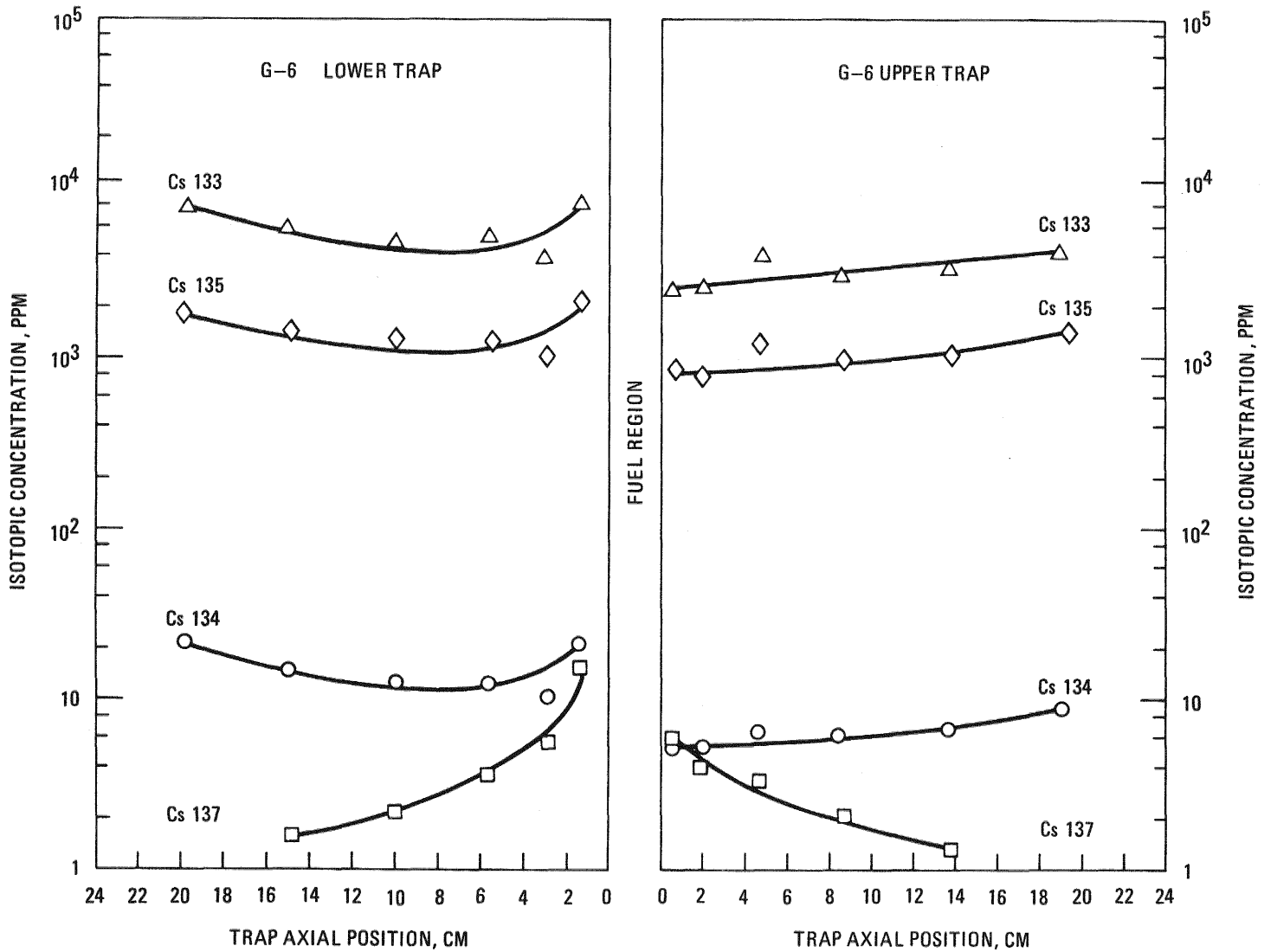

Fig. 14. Axial cesium concentration profiles for F-1 fuel rod G-6 charcoal traps

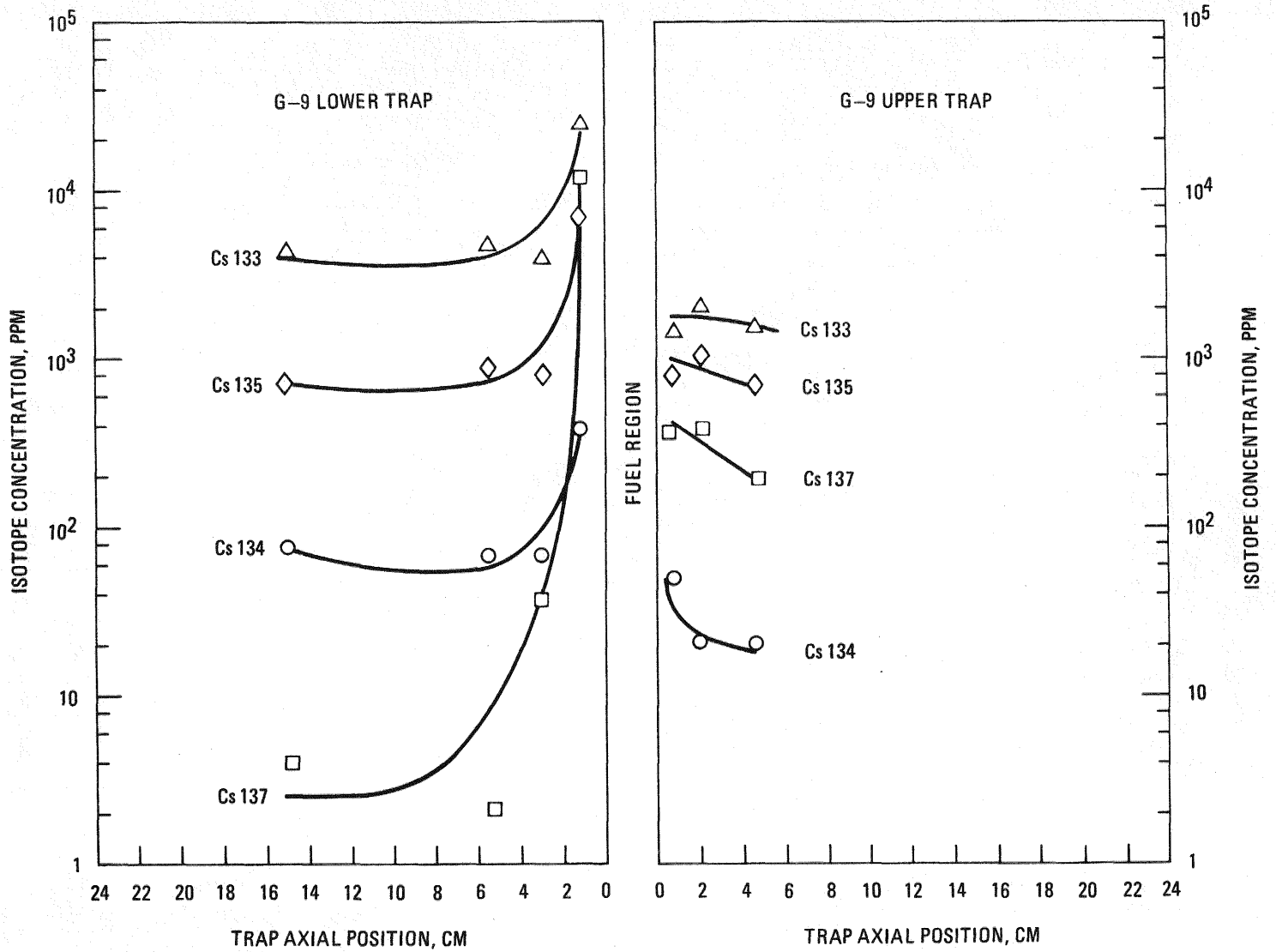

Fig. 15. Axial cesium concentration profiles for F-1 fuel rod G-9 charcoal traps

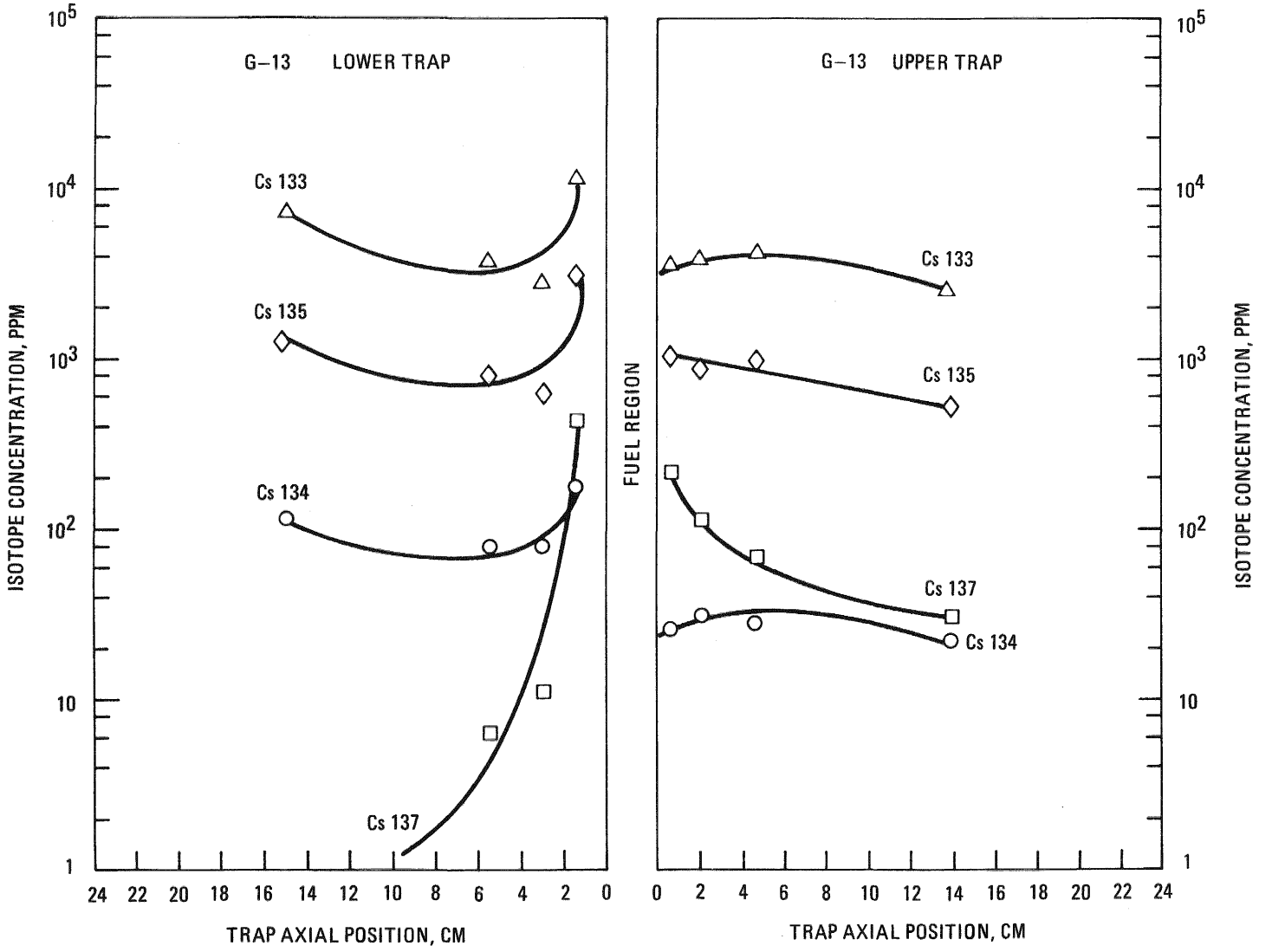

Fig. 16. Axial cesium concentration profiles for F-1 fuel rod G-13 charcoal traps

EBR-II spectrum are equal, the increased Cs-133 loading can only be attributed to enhanced R/B and/or transport of the longer half-life Xe-133 precursor.

3. The far steeper slope of the Cs-137 distribution in the charcoal trap indicates that decay of the short-lived transporting gaseous species is effective in reducing penetration of Cs-137 into the terminal sections of the trap. Since charcoal is known to essentially quantitatively retain cesium at temperatures up to ∿1000°C, the observed Cs-137 distribution indicates the equilibrium Xe-137 profile in the trap during reactor operation and shortly thereafter.

It does not appear possible, however, to state conclusively that Cs-137 is not transported beyond the blanket region as the vapor species. Although the observed distributions in F-1 rods can be adequately explained assuming precursor xenon transport, concomitant migration of vapor species cannot be excluded by the data at hand. Proof of vapor phase migration may yet come from analyses of cesium axial profiles in the axial blankets, which are now in progress. Results of analyses to date have shown only that the axial and radial profiles of all cesium isotopes in the first blanket pellet are relatively flat[20].

The long-lived Kr-85/Rb-85 and Kr-87/Rb-87 chains exhibit behavior similar to that of the long-lived xenon/cesium chains (Figs. 17, 18). Rubidium concentrations in the traps are lower than cesium concentrations because of the shorter half-lives of the gaseous precursors and slightly smaller fission yields. In spite of the fact that the alkali metal concentrations in the charcoal traps of the sealed rods are expected to be significantly higher than those in vented GCFR rods, the total alkali metal loadings are still in the milligrams of metal per gram of charcoal range. At these concentrations, the energy of adsorption is still high, and the charcoal remains highly retentive and will provide a significant delay in the release of cesium from GCFR rods.

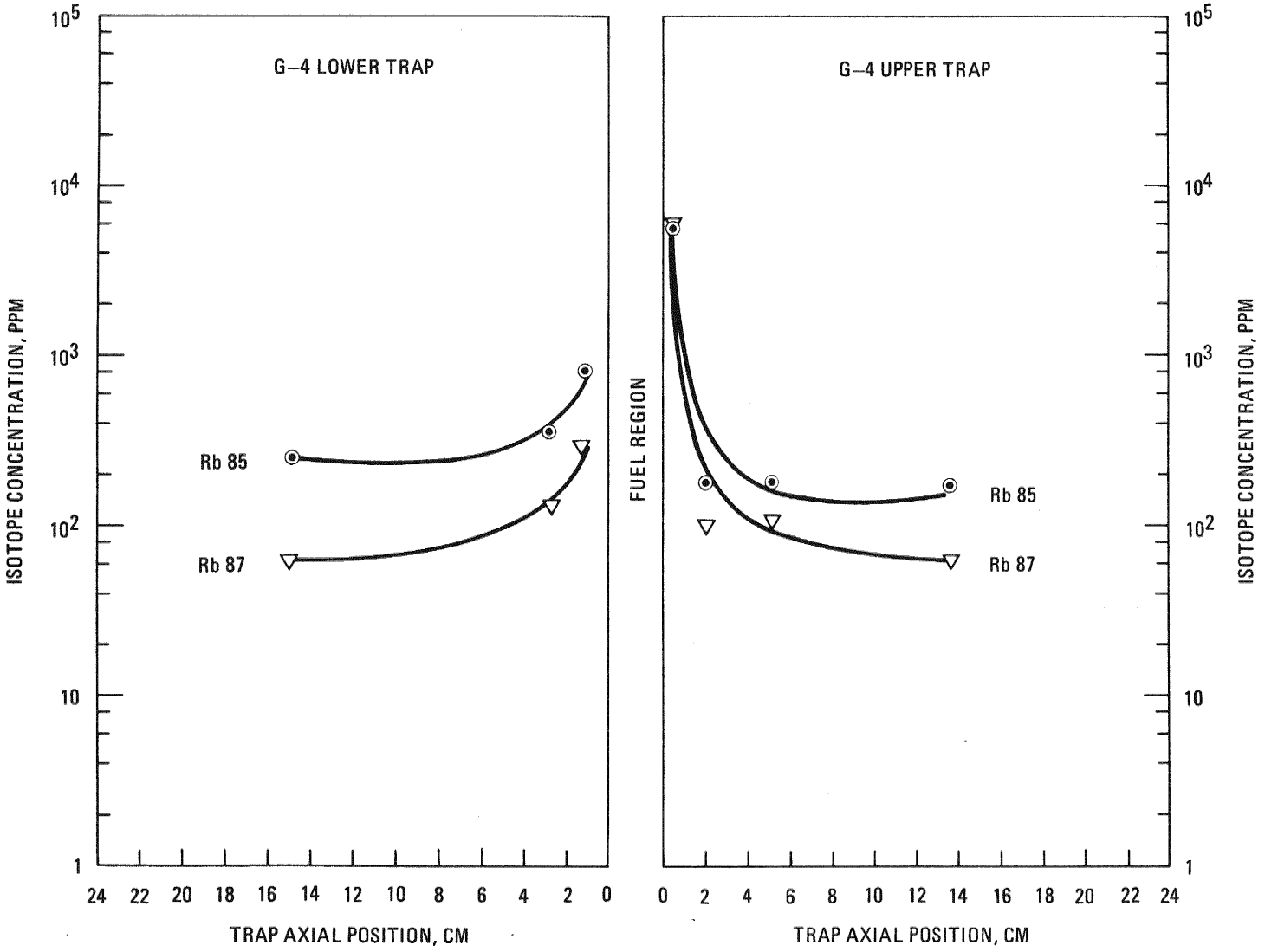

Fig. 17. Axial rubidium concentration profiles for F-1 fuel rod G-4 charcoal traps

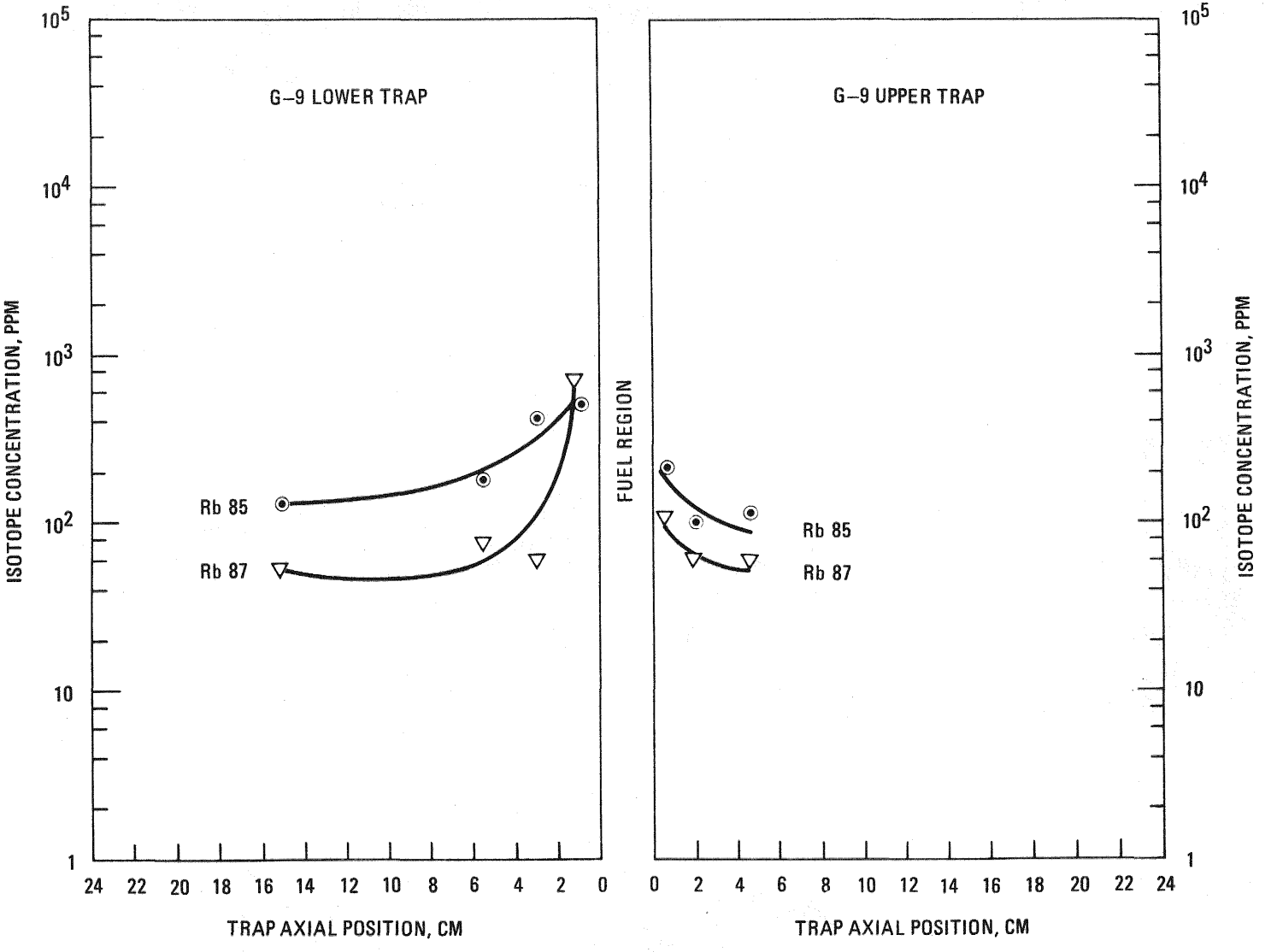

Fig. 18. Axial rubidium concentration profiles for F-1 fuel rod G-9 charcoal traps

CONCLUSIONS

The elements bromine, iodine, krypton, xenon, rubidium, and cesium are involved in the transport of fission products in fast breeder reactor fuel rods. The heavy mass region of the fission yield spectrum involving iodine, xenon, and cesium is of primary importance because of the half-lives and fission yields of the dominant mass chains. The low-mass elements must be considered, however, since they add to the total fission product inventory in the blanket and charcoal trap regions. All these elements take part in the transport process; the noble gases are clearly involved in transport to all portions of the fuel rod and are principally (perhaps solely) responsible for activity vented from rods. The volatile species iodine and cesium are known to be responsible for transport primarily to the fuel-blanket interface, where enhanced concentrations are found, and also presumably some distance into the blanket region. Bromine and rubidium are expected to behave similarly, but to a lesser degree. The volatile species is unknown; Cs, CsI, CsBr, Cs_2O, and CsOH (and the analogous rubidium compounds) are possible candidates. Some evidence (interaction with UO_2) points toward Cs or Cs_2O.

Noble gas transport is responsible for essentially all migration of the 133 and 135 mass chains to the charcoal traps in both sealed and vented rod irradiations. Xe-137 is thought to be the predominant transporting nuclide for the 137 mass chain; however, conclusive evidence for or against some volatile species migration is absent and may not be obtainable. Vented rod irradiation experiments yield data on R/B and V/B for noble gases and iodine during reactor irradiation; sealed rod irradiations provide only data on final fission product distributions during post-irradiation examination. The migrating species must be inferred.

The use of Cs-137 gamma activity as a monitor for total cesium distribution in a fuel rod is misguided, particularly since the different transport mechanisms induce an isotopic fractionation between the 137 mass chain

and the 133 and 135 mass chains. Cs-134 gamma activity is a more suitable monitor for approximately two-thirds of the total cesium distribution. Alkali metal loadings in the charcoal traps of vented GCFR fuel rods are expected to remain in the concentration range where the adsorption energy is high, and the charcoal will significantly delay the release of cesium from the rod.

ACKNOWLEDGMENTS

The authors wish to acknowledge the efforts of the principal experimenters, A. W. Longest and J. A. Conlin of ORNL, for their dedicated work on the GB-10 experiment. This experiment was carried out as a cooperative effort between ORNL, ANL, and GA.

REFERENCES

1. A. R. Veca et al., "Fuel Element Design for the 300 MW(e) Gas-Cooled Fast Breeder Reactor," Nucl. Eng. Design 40, 81 (1977).

2. M. Peehs, J. Lindgren, and P. Moser, "Gas-Cooled Fast Breeder Core Element Fabrication Technology," Nucl. Eng. Design 40, 101 (1977).

3. R. J. Campana, "Pressure Equalization System for Gas-Cooled Fast Breeder Reactor Fuel Elements," Nucl. Technol. 12, 185 (1971).

4. J. R. Lindgren et al., "I: Irradiation Experiments in the Development of a Vented, Helium-Cooled Fast Breeder Reactor Fuel Design," and H. Euringer et al., "II: Irradiation of GCFR Test Fuel Bundles in the BR-2 Helium Loop, Mol," in Proceedings of the International Conference on Fast Breeder Reactor Performance, March 5-8, 1978, Monterey, California.

5. S. Katcoff, "Fission Product Yields From Neutron-Induced Fission," Nucleonics 18, 201 (1960).

6. G. R. Crocker, "Fission Product Decay Chains: Schematics with Branching Fractions, Half-Lives, and Literature References," U.S. Naval Radiological Defense Laboratory Report USNRDL-TR-67-111, October 17, 1967.

7. S. Langer et al., "Volatile Fission Product Migration and Plateout in GCFR Rod Irradiations," Trans. Am. Nucl. Soc. 15, 850 (1972).

8. S. Langer et al., "The Behavior of Volatile Fission Products in GCFR Fast Flux Irradiation," Trans. Am. Nucl. Soc. 17, 219 (1973).

9. L. A. Neimark et al., "Performance of Mixed Oxide Fuel Elements to 11 A/O Burnup," Nucl. Technol. 16, 75 (1972).

10. R. A. Karnesky et al., "Cesium Migration in Mixed-Oxide Fuel Pins," Trans. Am. Nucl. Soc. 22, 229 (1975).

11. J. R. Lindgren et al., "Irradiation Testing in the Development of Gas-Cooled Fast Breeder Reactor Fuel Elements," J. Brit. Nucl. Energy Soc. 12, 395 (1973).

12. A. W. Longest and J. A. Conlin, "Results from Irradiation of Vented GCFR Fuel Rods in the GB-9 and GB-10 Capsule Experiments," Oak Ridge National Laboratory Report ORNL-5258, September 1978.

13. J. Belle (ed.), Uranium Dioxide: Properties and Nuclear Applications, USAEC, Washington, D. C., July 1961.

14. J. R. Findlay et al., "The Emission of Fission Products from Uranium-Plutonium Dioxide During Irradiation to High Burnup," J. Nucl. Mater. 35, 24-34 (1970).

15. M. C. Billone et al., "The LIFE-III Fuel-Element Performance Code," ERDA Report 77-56, Argonne National Laboratory, July 15, 1977.

16. K. H. Chang, M. P. LaBar, and R. J. Campana, "Modelling of Fission Gas Release in the GCFR Vented Fuel Rod," in Proceedings of the International Conference on Fast Breeder Reactor Performance, March 5-8, 1978, Monterey, California.

17. S. Langer, G. Buzzelli, and P. W. Flynn, "Postirradiation Examination of the Charcoal Trap in Irradiation Capsule GB-9," ERDA Report GA-A13298, General Atomic Company, May 28, 1975.

18. K. H. Chang and M. P. LaBar, "Fuel Cladding Mechanical Interaction in Irradiated GCFR Mixed-Oxide Fuel Rods," in Proceedings of the International Conference on Fast Breeder Reactor Performance, March 5-8, 1978, Monterey, California.

19. S. Langer and G. Buzzelli, "Cesium Transport and Isotopic Fractionation in Fuel Rods (IV)," Trans. Am. Nucl. Soc. 27, 232 (1977).

20. C. E. Johnson, Argonne National Laboratory, private communication, October 1978.